

CompleteSCAN: Genetic parameters of slaughter quality traits measured on whole or live Atlantic salmon

Final report

Anne Kettunen, Turid Mørkøre, Nils Kristian Afseth, Dennis Brandborg Nielsen, Troels Thorsen Mørch, Hooi Ling Khaw, Hooman Moghadam and Borghild Hillestad





Nofima is a business oriented research institute working in research and development for aquaculture, fisheries and food industry in Norway.

Nofima has about 390 employees.

The main office is located in Tromsø, and the research divisions are located in Bergen, Stavanger, Sunndalsøra, Tromsø and Ås.

Main office in Tromsø:

Muninbakken 9–13
P.O.box 6122 Langnes
NO-9291 Tromsø

Ås:

Osloveien 1
P.O.box 210
NO-1433 ÅS

Stavanger:

Måltidets hus, Richard Johnsgate 4
P.O.box 8034
NO-4068 Stavanger

Bergen:

Kjerreidviken 16
P.O.box 1425 Oasen
NO-5844 Bergen

Sunnalsøra:

Sjølsengvegen 22
NO-6600 Sunndalsøra

Alta:

Kunnskapsparken, Markedsgata 3
NO-9510 Alta

Company contact information:

Tel: +47 77 62 90 00

E-mail: post@nofima.no

Internet: www.nofima.no

Business reg.no.:

NO 989 278 835 VAT



Creative commons apply until otherwise stated

Report

<p><i>Title:</i> Genetic parameters of slaughter quality traits measured on whole or live Atlantic salmon (CompleteSCAN)</p>	<p>ISBN 978-82-8296-645-0 (pdf) ISSN 1890-579X</p>
<p><i>Tittel:</i> Genetiske parametere for slaktekvalitetsgenskaper målt på levende eller hel Atlantisk laks (CompleteSCAN)</p>	<p><i>Report No.:</i> 28/2020</p>
<p><i>Author(s)/Project manager:</i> Anne Kettunen, Turid Mørkøre, Nils Kristian Afseth, Dennis Brandborg Nielsen (Danish Technological Institute- DTI), Troels Thorsen Mørch (DTI), Hooi Ling Khaw, Hooman Moghadam (Benchmark Genetics Norway) and Borghild Hillestad (Benchmark Genetics Norway)</p>	<p><i>Accessibility:</i> Open</p>
<p><i>Department:</i> Breeding and genetics</p>	<p><i>Date:</i> 19.06.2020</p>
<p><i>Client:</i> Fiskeri- og havbruksnæringens forskningsfinansiering (FHF)</p>	<p><i>Number of pages and appendixes:</i> 65</p>
<p><i>Keywords:</i> Atlantic salmon, slaughter quality, computerized tomography, CT, genetic parameters</p>	<p><i>Client's ref.:</i> FHF: 901491</p>
<p><i>Summary/recommendation:</i> See chapter 1</p>	
<p><i>Summary/recommendation in Norwegian:</i> Se kapittel 1</p>	

Preface

This project was financed by FHF, Norwegian Seafood Research Fund (project number 901491).

Table of Contents

1	Summary	7
1.1	Summary in Norwegian	8
2	Introduction.....	9
2.1	Project background	9
2.2	The scope of the project.....	10
2.3	Organisation of the project	11
3	Aim and objectives.....	12
3.1	Main aim.....	12
3.2	Objectives	12
3.3	Benefits for the industry.....	12
4	Project execution	14
5	Findings, discussion and conclusion	15
5.1	WP1: Measure and record slaughter quality traits by manual dissection of fish at test slaughter.....	15
5.1.1	Test slaughter, manual dissection and CT scanning of dead fish	15
5.1.2	CT scanning of live fish	17
5.1.3	Results: production traits	18
5.1.4	Results: fillet quality traits.....	19
5.1.5	Conclusions from WP1	21
5.2	WP2: Measure and record slaughter quality traits on whole dead and live fish using a medical CT scanner.....	22
5.2.1	Background.....	22
5.2.2	Collection of data and scanning protocol.....	22
5.2.3	Fat in salmon	26
5.2.4	Detection of OWI's	28
5.2.5	Analysis of organs.....	33
5.2.6	Pigmentation	35
5.2.7	Melanin spots	35
5.2.8	Gaping.....	35
5.2.9	Conclusions for WP2.....	35
5.3	WP3: Measure pigmentation on whole, slaughtered fish.....	36
5.3.1	Background.....	36
5.3.2	Pigmentation: dead fish	36
5.3.3	Discussion and conclusions on pigmentation measurements, dead fish.....	39
5.3.4	Pigmentation: live fish	40
5.4	WP4: Estimation of genetic parameters and genome wide association study	41
5.4.1	Genetic parameters for production and fillet quality traits from manual slaughter	41
5.4.2	Genetic correlation manual vs CT on dead and live fish	56
5.4.3	Genome-wide association study and genomic analysis of live fish CT scans.....	56
5.4.4	Discussion and conclusions for WP4	59

6 Main findings 60

7 Deliverables 61

8 Acknowledgements 62

9 Literature 62

1 Summary

Genetic evaluation of slaughter quality of Atlantic salmon (*Salmo salar*) is based on resource demanding test slaughter of siblings of the breeding candidates. This method gives limited genetic improvement of slaughter traits due to the type of information and measurement error of the phenotypes.

In CompleteSCAN project, a two-stage approach was used to assess the possibility of utilizing novel phenotypes from CT scanning as selection criteria for slaughter quality of salmon.

First stage focussed on coupling manual dissection phenotypes to CT phenotypes in dead fish. First stage included also feasibility studies to 1) use CT scanning to detect quality traits in fillet and 2) quantify pigmentation of salmon flesh through skin with NIR (Near infrared spectroscopy) based Qpoint method and SORS (Spacially offset Raman spectroscopy) technology. Second stage focused on optimizing logistics and execution of CT scanning of live fish.

A custom-made program was used to remove the organs, head and tail by applying a virtual three-dimensional mask. Individual scans were further segmented into different types of tissues based on the x-ray absorption properties of the tissues. CT phenotypes were converted to weight traits by multiplying volumes with the corresponding tissue densities.

CT traits of dead fish showed moderate to high heritabilities (except bone fraction of whole and gutted fish). CT phenotypes from dead fish were genetically highly correlated to the corresponding dissection traits. Fillet fat percentage estimated with CT reliably ranks individuals relative to the traditionally used NIR fat phenotype. High correlation between the chemical composition of the fillet fat and fat content based on NIR is well known, and this interrelationship was also confirmed with the current material.

Feasibility assessment of the CT scans showed that fillet quality traits of melanin spots, gaping and pigmentation cannot be detected using CT scans. Importantly, the same CT scans can be used to define many, also novel, phenotypes, by adjusting the software. This said, other image technologies, may be more suitable for registration of many of these traits, such as external deformities and wounds.

Qvision NIR scanner showed its feasibility for rapid scanning of pigments in salmon fillets. Qpoint did not provide robust models for quantification of pigments in whole fish. The handheld SORS device from Agilent Technologies, Inc did not provide enough resolution and laser power to penetrate deep enough into the salmon tissue. Consequently, SORS did not allow quantitative information of the pigments in whole salmon to be obtained. Only lipid information from the adipose tissue beneath the skin could be obtained.

Operation time of the live fish CT scanning was on average 3.5 min per scan. Practical solutions relative to sedation, transport to CT scanner, and fixative to guarantee good quality scans without movement were successful. Mortality connected to the operation was 10 %. Live fish CT scanning verified moderate estimates of heritability for the CT phenotypes.

The largest potential lies in using live fish CT scanning to provide precise phenotypes of high value cuts measured directly from breeding candidates. This allows minimizing the number of experimental animals and increased accuracy of the estimated breeding values, and given moderate heritabilities, increased genetic gain.

1.1 Summary in Norwegian

Genetisk evaluering av slaktekvalitet hos atlantisk laks (*Salmo salar*) er basert på ressurskrevende testslakt av søsken til avlskandidatene. Denne metoden gir begrenset genetisk framgang ettersom egenskaper er registrert på slektninger og fordi registreringene har betraktelige målefeil.

CompleteSCAN-prosjektet brukte en tottrinns tilnærming for å vurdere muligheten for å bruke nye fenotyper fra CT-skanning som seleksjonskriterier for slaktekvalitet hos laks.

Første trinn fokuserte på å koble manuelle disseksjonsfenotyper til CT-fenotyper hos død fisk. Første trinn undersøkte også muligheter for å 1) bruke CT-skanning for å oppdage melaninflekker i fillet og 2) kvantifisere pigmentering av laksekjøtt gjennom hud med NIR-basert Qpoint-metode og SORS-teknologi (Spatially offset Raman spectroscopy). Andre trinn fokuserte på å optimalisere logistikk og utførelse av CT-skanning av levende fisk

Et skreddersydd program ble brukt til å fjerne organer, hode og hale. Individuelle skanninger ble videre segmentert i volum av forskjellige typer vev basert på røntgenabsorpsjonsegenskapene til vevene. Volumfenotyper ble omdannet til vekt ved å multiplisere volumer med tilsvarende vevstettheter.

CT-egenskaper fra testslakt viste moderat til høy arvegrad (unntatt beinfraksjon av hel og sløyd fisk). CT-fenotyper fra død fisk var genetisk sterkt korrelert med de tilsvarende egenskapene fra test slakt. Fettprosent, beregnet med CT, rangerer individene pålitelig i forhold til den tradisjonelt brukte NIR-fettfenotypen. Høy korrelasjon mellom den kjemiske sammensetningen av filletfettet og fettinnholdet basert på NIR er tidligere dokumentert, og dette forholdet ble også bekreftet med det aktuelle materialet.

Analysene av CT-bilder viste at filletkvalitetstrekk som melaninflekker, spalting og pigmentering ikke kan påvises i CT-skanninger. Samme CT-skanning kan brukes til å måle mange ulike fenotyper, også fenotyper som ikke var definert da skanningen ble gjennomført, ved å tilpasse software. Andre metoder, slik som hyperspektral avbildning, kan være mer egnet for registrering av mange trekk, slik som ytre deformiteter og sår.

Qvision er en metode som gir et nøyaktig mål på pigmenter i laksefileter gjennom rask skanning. Qpoint egnet seg ikke for kvantifisering av pigmenter i hel fisk. Den håndholdte SORS-enheten fra Agilent Technologies, Inc ga ikke nok oppløsning og laserkraft til å trenge dypt nok inn i laksevevet. Derfor ga ikke SORS kvantitativ informasjon om pigmentene i hel laks, bare lipidinformasjon fra fettvevet under huden.

Gjennomsnittlig medgått tid for CT-skanning av levende fisk var 3.5 minutt. Praktiske løsninger i forhold til bedøving, transport til CT-skanner, fiksativ for å garantere CT-bilder av god kvalitet uten bevegelse, var vellykkede. Dødeligheten knyttet til operasjonen var 10 %. CT-skanning med levende fisk bekreftet moderate estimater av arvegrad for CT-fenotypene.

Det største potensialet for CT-skanning av levende fisk er presise fenotyper målt direkte på avlskandidatene. Dette tillater minimering av antall forsøksdyr og økt nøyaktighet på de estimerte avlsverdiene, og gitt moderate arvegrader, økt genetisk framgang.

2 Introduction

2.1 Project background

Precise, effective and objective measurements of economically important traits that express genetic variation are prerequisites for successful selective breeding program. Salmon selective breeding program has been and still is the cornerstone of the Norwegian aquaculture. Benchmark Genetics Norway (BGN), our collaborator in this project, is one of the four breeding companies currently managing a salmon breeding program and selling fertilized ova to fish farmers.

Salmon breeding companies have typically broad breeding goals combining economically important traits, such as growth, carcass quality, disease and parasite resistance. Genetic improvement of carcass and quality traits is a continuous work across all salmon breeding companies. The goal is to assure fast growing fish with high fillet yield of high technological and sensory quality.

Currently, as part of a sustainable breeding program, BGN performs a large-scale sib-test to assess the genetic value of the breeding candidates relative to their slaughter quality. A group comprising of 6-10,000 individually tagged full-sibs of the breeding candidates are set out in the sea and reared under commercial conditions. When fish reaches the harvest weight of approximately 5 kg, they are harvested, measured and manually dissected to record traits such as round weight, gutted weight, fillet weight, fillet fat percentage, sex and state of sexual maturation. Tissue samples are collected for genotyping. The phenotypes of the test-group are then related, through pedigree and genomic information, to the breeding candidates, and breeding values are estimated.

The current evaluation method has two main disadvantages. First, production, rearing and slaughtering the yearly test group comes with a great cost, time and effort. Production expenses include the costs connected to production itself, e.g., hatchery, PIT-tagging, feed throughout the production cycle, cage rental and rearing. Additionally, there is a great cost connected to the massive harvest, slaughter and dissection process, where an entire slaughterhouse with workers are needed for a whole week. Genomic evaluation is coupled with an additional cost of genotyping.

Second, the potential of genetic improvement in slaughter quality traits is somewhat limited. This in turn arises from two reasons. As the fish need to be sacrificed in the current assessment method, the valuable slaughter quality traits are only recorded in the test group, that is on relatives, not on the breeding candidates themselves. To compensate the inaccuracy of the indirect evaluation, the number of test fish is maximised. Additionally, manual dissection phenotypes are coupled with measurement error as parts of the muscles remain on the head and on the bones and will be recorded as waste. This results in error in gutted, headless and fillet weight of the carcass, and is often operator dependent.

To investigate the possibility to measure slaughter traits directly on live breeding candidates and avoid manual dissection, we wanted to utilize new cutting-edge technologies, like computed tomography (CT) scanning and spatially offset Raman spectroscopy (SORS) in this project. Direct evaluation of breeding candidates would improve the accuracy of genetic evaluation significantly and reduce the number of test fish to be used in the breeding program.

CT scanning has been used to calculate body composition of live selection candidates of Norwegian Landrace and Duroc boars, for traits such as growth rate of muscle and fat, and leanness (Gjerlaug-

Enger et al. 2012). The study showed high accuracy of CT data and proved the potential of incorporating new traits as selection criteria. Earlier studies have reported that CT scans accurately predict fat and protein percentage in rainbow trout (Gjerde 1987) and Atlantic salmon (Rye 1991), but so far this methodology is not implemented in salmonid breeding programs. Traits derived from CT scans have had moderate to high heritability in pigs and sheep (Gjerlaug-Enger et al. 2012; Maximini et al. 2012) when compared to traits obtained from traditional approaches. This gives promise to comparable estimates for CT derived slaughter traits in Atlantic salmon.

Phenotypes from CT scans are created using 3D image analysis of the different x-ray absorption properties of different tissues. Image analysis software is used to extract the tissue distribution which also enables definition of novel post-scan phenotypes. Such approach remedies simultaneously several disadvantages of manual dissection: cost of labour and materials, and operator dependence.

In addition to the carcass composition, quality traits such as frequency of dark spots in fillet and fillet pigmentation are significant for the salmon industry from the economic and consumer acceptance point of view. It has been speculated whether the dark spots in the fillet are breeding related. Dark spots are commonly located cranio-ventrally, under the abdominal peritoneum and the ribs. This makes them invisible to the human eye without removing peritoneum and ribs. They are characterized with accumulation of melano-macrophages, occasional formation of granulomas and substitution of skeletal muscle with scar tissue (collagen) (Mørkøre et al 2015; Holló et al. 2017). Tissue density differences between melanin spots and healthy tissue might enable detection of dark spots with CT scanner.

Pigmentation is another major quality feature of farmed salmon. Techniques used for measurement of pigmentation in the muscle include visible/near-infrared (VIS/NIR) spectroscopy or colour cameras. Measuring pigmentation in whole fish is strongly affected by the visible light absorption of the salmon skin, and prediction may not be accurate enough for breeding purposes. Raman spectroscopy gives a direct chemical fingerprint of pigments found in salmon. Recently, Nofima showed that a special type of Raman technique, namely spatially offset Raman spectroscopy (SORS), can be used to radiate through salmon skin and probe fatty acid and pigment features in muscle of round salmon (Afseth et al. 2014). In this project, we want to further evaluate the possibilities for quantitative analysis of pigmentation using Raman spectroscopy, and compare these findings with the state-of-the-art VIS/NIR spectroscopy.

The project assesses the use of new techniques on large scale phenotyping of Atlantic salmon relative to the slaughter quality, and if implemented in practice, these techniques would have significant multifaceted effect on the whole salmon industry.

2.2 The scope of the project

Project started 3/2018 and planned finalising and end reporting was set originally at 3/2020. Project received 7 863 000 NOK financing from FHF. An amendment was submitted in November 2019 due to significant delays in the project, more precisely the delay in CT scanning of the live fish due to technical difficulties. After the amendment, project end was postponed until 1st of June in 2020.

This project was a collaboration between Nofima, Benchmark Genetics Norway (BGN) and Danish Technological Institute, department Danish Meat Research Institute (DTI/DMRI). Nofima has been the

leading institute and responsible for work packages WP1, WP3 and WP4. BGN has provided the fish material and been responsible for the practical execution and collection of data for manual slaughter and live fish scanning. Additionally, BGN has been responsible for genotyping and executing genome wide association study (GWAS) as a part of WP4. DMRI has been responsible for WP2; the practical CT scanning, as well as all research and development regarding product/method aiming at CT phenotypes for genetic analysis.

2.3 Organisation of the project

The project was organized in four work packages:

1. WP1: Measure and record slaughter quality traits by manual dissection of fish at test slaughter
2. WP2: Measure and record slaughter quality traits on whole dead and live fish using medical CT scanner
3. WP3: Measure pigmentation on whole, slaughtered fish
4. WP4: Estimation of genetic parameters and genome wide association study

The project group originally comprised of Solomon Antwi Boison (project and WP4 leader), Turid Mørkøre (WP1 leader), Nils Kristian Afseth (WP3 leader) from Nofima and Paul Andreas Holger Dirac from DTI, DMRI (WP2 leader). In September 2018, Anne Kettunen from Nofima replaced Solomon Antwi Boison as project and WP4 leader.

BGN provided the fish for the project, arranged the practical logistics for phenotyping at manual slaughter and live fish registration (responsible persons Borghild Hillestad and Hooman Moghadam). These operations were the core of the whole project, alone responsible for producing all the phenotypes for further analysis. CT scanning, method development and segmentation of CT scans for CT-phenotypes, as well as assessment/feasibility analysis were done by Dennis Brandborg Nielsen and Troels Thorsen Mørch.

Genotyping was organized by BGN using Nofima-BGN co-owned custom-made 55K Affymetrix genotyping array, NOFSAL03. GWAS was performed by Borghild Hillestad and Hooman Moghadam at BGN.

The reference group comprised of Håvard Bakke, Borghild Hillestad and Hooman Moghadam from BGN. Observer of the reference group and FHF contact person was Kristian Prytz.

3 Aim and objectives

3.1 Main aim

The main aim of the project was to be able to measure slaughter quality traits on whole and live fish utilizing highly developed techniques to improve and advance the breeding program for Atlantic salmon.

3.2 Objectives

- To assess whether phenotypes for slaughter quality measured by CT scanning are more precise than those achieved with traditional test-slaughter and manual dissection
- To assess whether pigmentation can be reliably measured by SORS methodology instead of NIR/VIS and chemical analysis
- Estimate heritability of body composition and fillet quality traits (melanin spots, pigmentation, fat content, etc.) in the fillet and assess whether those can be detected with CT scanning
- Search for genetic markers for the new phenotypes and compare and correlate those with manually registered traits

3.3 Benefits for the industry

This project was expected to create benefits for the salmon aquaculture industry on different levels. Overall, it was expected that the project will contribute with increased knowledge on new technologies that will increase the precision of registration of slaughter traits, necessary for improved quality of the aquaculture salmon. If feasible, implementation of these new technologies may turn the yearly sib-evaluation unnecessary, and significant reduction of management costs are expected for the breeding companies.

The Project was expected to result in development of precise, effective and non-invasive technologies for slaughter evaluation of fillets, round dead fish and ideally also live fish. Increased genetic gain in important quality traits was expected to be achieved through two channels. More precise recording of the slaughter quality traits, and potentially new phenotypes, could give more reliable genetic evaluation of biometric characteristics, chemical composition and appearance, and accelerate genetic gain. Additionally, direct measurement of the breeding candidates, if feasible, was expected to give an additional increment to the genetic gain. In long term, the project could contribute to decreased number of experimental animals, improved animal welfare as consequence of selection for more robust salmon with less deformities, increased growth and subsequently shorter time in the sea, and ideally reduced parasite and disease pressure. All the above will benefit the salmon industry from the breeding company to fish farmers.

Method innovations have large potential as tools for quality control in the salmon industry; new technological innovations could be used to detect dark spots in fillet and gaping, which both have large economic importance.

Altogether, the project was expected to improve the consumer acceptance due to possibilities to define more diverse breeding goal, improved product quality and animal welfare.

Project deliverables were aligned with the main aim, objectives and expected benefits to the industry. In particular, assessment of the feasibility of the use of the new technologies (CT, SORS) were in focus. Validation of the new technologies against existing routine evaluation was the core of the project.

Overview of the organization of the project together with the deliverables is presented in Figure 1.

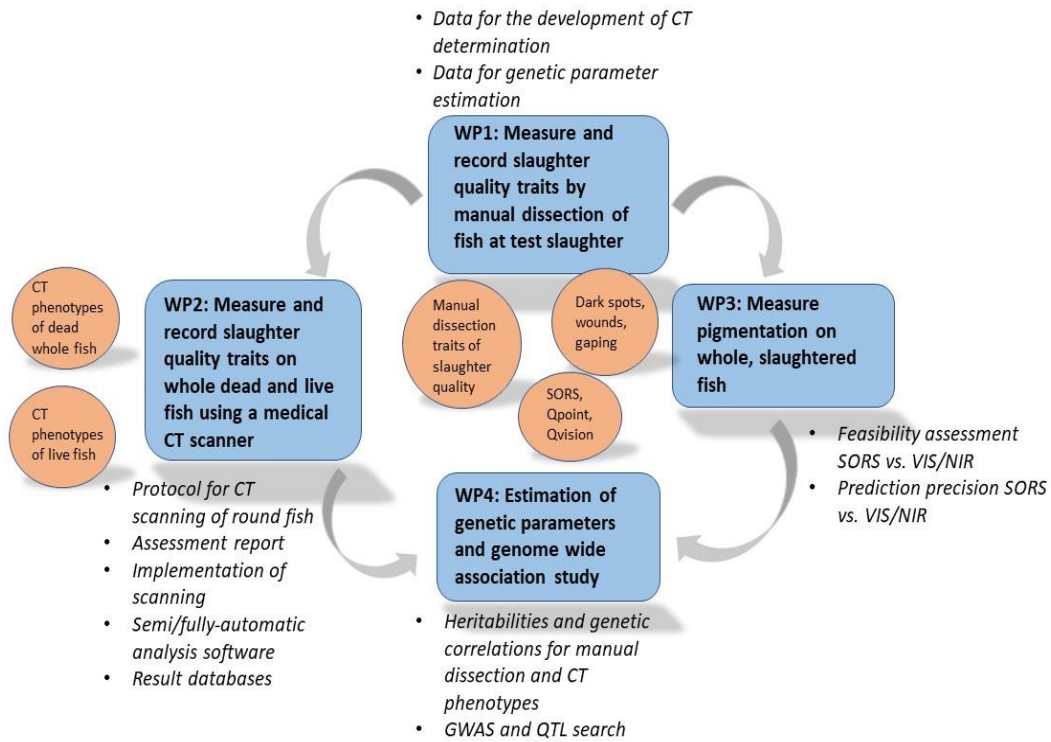


Figure 1 Overview of the structure of CompleteSCAN project with deliverables.

4 Project execution

Two year-classes of BGN/SalmoBreed material was used in this project. In March 2018 slaughtered SalmoBreed material from year-class 2016 was registered and CT scanned. The original plan was to scan live breeding candidates that were to be culled from the same year-class during spring 2019. Unfortunately, due to technical difficulties this trial needed to be postponed until November 2019, where year-class 2018 test-slaughter fish were successfully CT scanned.

For the objectives of the study, an experimental design was chosen that would connect the manual slaughter information to dead-fish CT scanning, and by using close relatives, to live fish CT scanning. This would give us reliable indication of the reliability of CT scanning of live breeding candidates compared to what their slaughter quality would be at slaughter. The plan was to utilize both pedigree and genomic information to connect the groups to unravel the genetic interrelationships between phenotypes from the different registration methods. Due to complications mentioned above we utilized year-class 2018 which has limited pedigree connections to the year-class 2016 (see Table 2 in section 5.1.1). Additionally, tissue samples from the manual slaughter in 2018 (year-class 2016) were un-optimally handled and stored, leading to poor quality DNA and failure in genotyping. Consequently, the genomic relationships to patch up the weak pedigree connection between these two scanning are not available.

In particular, the attempt was to use non-invasive methods to detect quality traits (fillet yield, dark/melanin spots, pigmentation, gaping, defects/damage) in salmon. CT scans from the first stage of the study, manual slaughter, proved that the melanin spots are undetectable in the CT scans (section 5.2.7). Additionally, we did not find significant additive genetic variation in melanin spots (section 5.4.1). Further exploring of the melanin spots were therefore abandoned in the project.

Similarly, we pursued the use of SORS technology using a hand-held instrument during the manual slaughter to detect pigmentation in flesh. Unfortunately, this did not allow quantification of the pigments in whole salmon (section 5.3). Consequently, the use of this technology was abandoned from the live fish scanning.

5 Findings, discussion and conclusion

5.1 WP1: Measure and record slaughter quality traits by manual dissection of fish at test slaughter

5.1.1 Test slaughter, manual dissection and CT scanning of dead fish

Test slaughter of year-class 2016 family material, progeny of 144 sires and 276 dams, was conducted between 5th and 9th of March 2018 at Austevoll Laksepakkeri. The main goals of this massive operation were:

- i) To CT scan 2,000 dead, whole fish
- ii) To scan as many fish as possible within the 5-day time limit, using Qpoint and SORS Raman technology
- iii) As part of Benchmark Genetics Norway's breeding program, to manually dissect, weigh, record, VIS/NIR-scan and DNA sample a testing group, consisting of approximately 6,000 PIT-tagged fish with pedigree, representing SalmoBreed nucleus families and lines of 2016 year-class, as well as StofnFiskur nucleus families of 2015 year-class (cohort 2)
- iv) To score, grade and record melanin spots, wounds and gaping, as well as sample melanin tissues for as many candidates as possible given the time constraint

The fish group was reared at LetSea and harvested at Fiskekroken, then deep-frozen a month prior to the transportation to Austevoll Laksepakkeri for defrosting and processing. Out of the 276 families registered for production traits, 176 families of SalmoBreed strain were selected for the CT scanning for the project. Further, 104 families, ten candidates per family from the CT scanned families, were marked out to be recorded with the Qpoint and SORS. Test slaughter and manual dissection resulted in registrations of **production traits** (N=3,044) and **fillet quality traits** (gaping, melanin spots, fillet deformity N=2005) and **CT phenotypes** (N=2,012). The details of the process of creating CT-phenotypes from scans and CT method development will be described in section 5.2. SORS measurements were conducted on 236 fish, and Qpoint on 680 fish, and analysis of that data will be presented in detail in section 5.3.

The fish were killed and frozen approximately one month prior to the registration, which may have affected registration of some of the fillet quality traits (see 5.1.4). At test-slaughter fish were thawed and registered for PIT-tag, sex, state of sexual maturity, round weight, gutted weight, deformities and wounds. Consequently, fish were filleted and trimmed, and registrations were done for fillet weight (both sides), fillet deformities, fillet pigmentation, fat percentage, gaping, and presence and severity of dark spots on the fillet. Based on the weight traits fillet yield traits were calculated. List of traits selected is presented in Table 1. The assembly of these phenotypic data was the core of the first phase of the project: method development and feasibility study for CT phenotypes (details in 5.2), assessment study for use of SORS methodology, and genetic parameters estimation for the same selection of traits (section 5.4).



Figure 2 Registration pipeline in the test slaughter and manual dissection.

Table 1 Traits registered in test slaughter and manual dissection.

Trait	Abbreviation	Information of the trait
Production traits		
Harvest weight	HWT	In gram
Body length	LGTH	In centimeter
Gutted weight	GWT	In gram
Fillet weight	FWT	In gram, both fillets combined
Fillet yield, gutted weight	FYGWT	In percentage, $\frac{FWT}{GWT} \times 100 \%$
Fillet yield, harvest weight	FYHWT	In percentage, $\frac{FWT}{HWT} \times 100 \%$
Fat percentage	FAT	NIR, %
Pigmentation	PIGM	VIS, mg kg ⁻¹
Wound present	WND	Binary trait with 0 and 1
Wound score	TWS	Wound scale, see text and Appendix 1
Fillet quality		
Gaping	GAP	Gaping scale, see text
Melanin score	MelSc	Melanin scale, see text
Presence of melanin	PMel	Binary trait with 0 and 1
Fillet deformity	FDef	Binary trait with 0 and 1

5.1.2 CT scanning of live fish

The second sampling took place at Bremnes Seashore from November 10-15, 2019. The aims of this sampling were

- i) To sedate and CT scan 2,000 live fish with as low mortality as possible
- ii) To harvest and perform a quality test for the entire group of approximately 8,800 fish by recording weight, length, deformities and maturation, as well as sampling for DNA
- iii) To fillet and trim 1,000 fish, select out 400 fillets, 200 pale and 200 red, and NIR scan for fat and pigmentation contents.

The two latter points were mainly performed as part of Benchmark Genetics Norway's breeding program, but also provided control information to the CompleteSCAN project. The families used for this study were selected to have the highest possible relation to the first dataset, as some of the families of 2016 and 2018 year-classes share grandparents, as shown in Table 2. CT scanned individuals originated from 200 families, and were parented by 99 sires and 108 dams from year-classes 2014 and 2015. Pedigree was traced back for 6 generations.

Table 2 *The pedigree relationships between different SalmoBreed subpopulations. Fish from year-classes 2016 and 2018 were used in this project.*

Generation	SalmoBreed year-classes			
F0	2001	2002	2003	2004
F1	2005	2006	2007	2008
F2	2009	2010	2011	
F3	2012	2013	2014	2015
F4	2015	2016	2017	2018
F5		2019	2020	

5.1.3 Results: production traits

Summary of the production traits from test slaughter and manual dissection (data collection presented in 5.1.1) is shown in Table 3. Please look at Table 1 for trait definitions.

Table 3 Summary statistics of the production traits from the manual slaughter.

Variable	N	Mean	Min	Max	SD	CV (%)
HWT (g)	2996	4165.22	1440.00	7400.00	798.16	19.16
LGTH (cm)	3009	65.05	47.00	80.00	4.18	6.43
GWT (g)	2935	3626.55	1120.00	6480.00	708.33	19.53
FWT (g)	2939	2202.15	490.00 ^a	4030.00	484.24	21.99
FYGWT	2869	60.53	47.20	75.60	4.97	8.20
FYHWT	2883	52.78	40.00	68.90	4.73	8.96
FAT	2872	18.50	11.80	27.20	2.18	11.76
PIGM	2847	5.09	2.60	7.70	0.82	16.19
WND	3044	0.47	0	1	0.50	107.1
TWS	3044	0.64	0	2	0.76	119.26
GAP	2005	5.56	0	10	2.65	47.71
MeIsc	2005	0.57	0	8	1.04	183.59
Number of melanin spots	2005	0.38	0	4	0.61	161.84
PMel	2005	0.32	0	1	0.47	146.58
FDef	2005	0.10	0	1	0.30	303.88

^a Production data: this fish only has fillet weight, spine weight and headless weight.

Weight traits

Harvest weight (HWT), body length (LGTH), gutted weight (GWT) and headless weight (not shown here) were recorded *prior* filleting. Fish was filleted and fillet weight phenotype was formed as a sum of both the fillets (FWT). The mean HWT was 4165 g and mean LGTH of 65 cm. For fillet yield, the means based on GWT and HWT were 60.5 % and 52.8 %, respectively.

Pigmentation

Description of the methods used to register pigmentation are presented in section 5.3.2.

Wounds

Both the location and severity of wounds were recorded from both sides of the fish. Total wound score (TWS) was created as the sum of the severity scores of all the wounds on a fish. The wound scoring system is presented in Appendix 1. TWS was condensed into three phenotypes for genetic analysis: TWS=0 (no wounds present), TWS=1-3, and TWS≥4. In this scoring system, different number and severity could lead into the same phenotype. Additionally, a binary trait, “wounds present” (0 = absent, 1 = present) was used in the genetic analysis.

A total of 1,418 fish were affected by wounds (46 %). There were no significant differences in registrations between operators. Out of the fish with wounds, over 30 % had only one wound, and 10 % two wounds. Highest frequency of wounds was observed in the mid-area of the fish (Table 4). Less than 5 % of the wounds were classified with score 8. Majority of the wounds were scored either 1 or 2 (75 %) (Table 4, Figure 3). The cause and possible heritability of wounding is complex and

unknown. Possible causes of wounds include mechanical damage, damage caused by cleaner fish, viral/bacterial infections, and combinations of them.

Table 4 Proportion of the wounds in different areas and severity classes of the total wounds recorded in the manual dissection.

	Position								Total	
	Dorsal		Mid		Belly		Head	Tail		
	Front (R1)	Back (R2)	Front (M1)	Back (M2)	Front (B1)	Back (B2)	(H)	(S)		
Score	1	2.52 %	2.25 %	9.06 %	9.22 %	3.70 %	4.13 %	1.50 %	6.32 %	38,71 %
	2	2.73 %	2.95 %	7.29 %	10.29 %	2.47 %	4.56 %	1.29 %	4.39 %	35,98 %
	4	1.61 %	1.39 %	4.72 %	5.57 %	2.47 %	2.95 %	0.16 %	1.55 %	20,43 %
	8	0.48 %	0.16 %	1.55 %	1.82 %	0.43 %	0.27 %	0.05 %	0.11 %	4,88 %
Total		7,34 %	6,75 %	22,62 %	26,90 %	9,06 %	11,90 %	3,00 %	12,4 %	

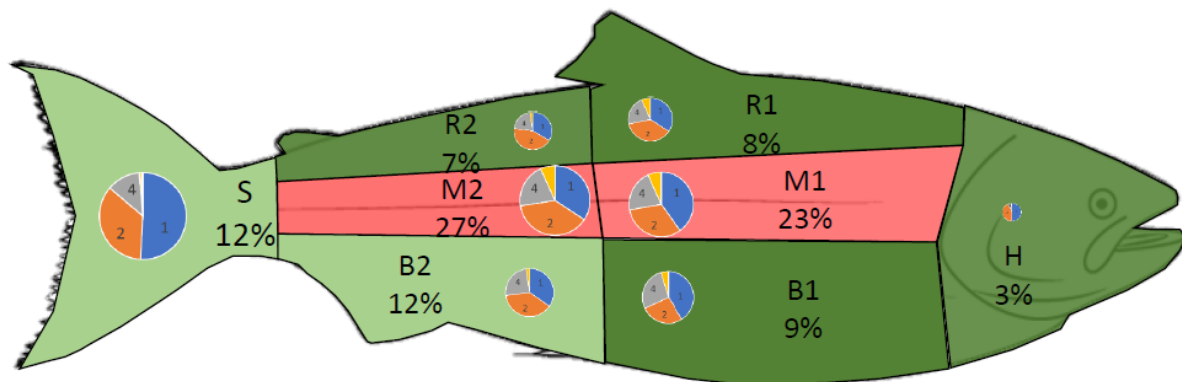


Figure 3 Wound areas and frequencies of wounds in different areas in test slaughter.

5.1.4 Results: fillet quality traits

For the fillet quality data, registered in connection of the manual dissection (data collection presented in 5.1.1), all phenotypes were recorded on left and right fillets. Preliminary analyses showed high correlations between left and right fillet quality traits. Consequently, combined fillet quality phenotypes were formed by summing up phenotypes from the individual fillets: for example, the gaping score of the fish was the sum of the gaping scores from left and right fillet.

Gaping

Gaping was scored by one person only according to the system by Andersen et al. 1994 (Figure 4). Typically gaping is scored when *rigor mortis* is passed, approximately 4 days after slaughter. In this experiment, the fish was slaughtered one month earlier, frozen and thawed for the manual dissection. Gaping in frozen fish is more severe than in fresh fish. Additionally, the thawing process was not constant over the sampling period, which causes additional variation in the gaping phenotypes. The average gaping score of this experiment was 5.56 (max. 10) (Table 3). There was a tendency of decreasing gaping score by sample day.

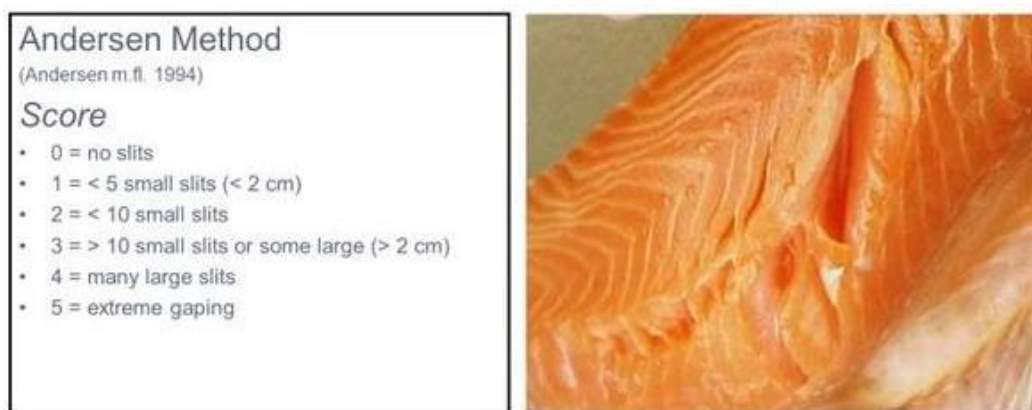


Figure 4 Gaping scoring system in the manual slaughter.

Fillet deformity

Fillet deformity was observed as changes in connective tissue on the fillet. If the fish has fused vertebrae this will cause white thickened areas on the midline of the fillet. Fillet deformity was defined as binary trait in genetic analysis (0/1).

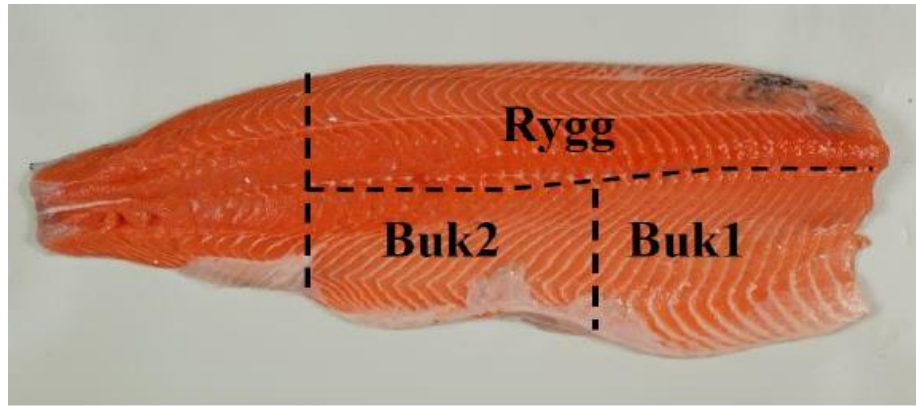
Dark spots

For melanin phenotypes, the position (Figure 5), melanin score, size of the spot both as the number of discolored muscle segments overlapped by the spot, and size in height x width (mm²), and color of the spot (dark, red) were recorded at test slaughter.

Melanin score was registered for 2,005 fish (Table 3) as the sum of melanin score of all dark spots in both fillets. Additionally, a binary melanin phenotype was formed: 0 = no melanin spots, 1 = melanin spot(s) present on any of the fillet was used in the genetic analysis. Out of the 3,044 registered fish 32 % had melanin on at least one of their fillets. Additionally, for 636 fish detailed information on the area covered by dark spots and the color of the spots was available. For detailed analysis, the phenotypes were either combinations of phenotypes over fillets (area or segment covered), or area phenotypes by the color of the spots over fillets (D=dark and R=red). There were 46 individuals that had both dark and red spots on their fillets. The descriptive statistics of this detailed analysis is presented in Table 5.

Table 5 Descriptive statistics for melanin spots in term of area (AREA, mm²) and number of segments covered (SEG) as the sum of all the spots or by the color of the spots (D=dark or R=red).

Variable	N	Mean	Min	Max	SD	CV (%)
AREA	636	279.5	1	2600	354.9	127.0
SEG	636	3.9	1	17	2.4	61.9
D – AREA	360	289.4	1	2080	316.4	109.3
D – SEG	360	4.0	1	13	2.1	50.9
R – AREA	323	227.7	1	2600	362.1	159.0
R – SEG	323	3.1	1	17	2.1	68.2



Score 1	Score 2, distinct <3cm	
Dark spots		
Small, 9102	Medium, 7126	Large, 9029, 6992
Amount of tissue available: 72g	Amount of tissue available: 260g	Amount of tissue available: 154g
Red spots		
Small, 9107	Medium, 7758	Large, 8375, 7930
Amount of tissue available: 22g	Amount of tissue available: 123g	Amount of tissue available: 170g

Figure 5 Assessment and location of melanin spots in manual slaughter.

5.1.5 Conclusions from WP1

Test slaughter and manual dissection, as well as CT scanning of dead fish (details in 5.2), were successfully executed. This dataset formed the core of the method and software development for CT scan segmentation as well as formed the basis for the feasibility studies in WP2. WP1 sampling was used to assess the potential of novel methods for quantification of pigmentation in whole fish in WP3. Additionally, WP1 successfully provided both production and CT data for WP4 and genetic parameter estimation.

5.2 WP2: Measure and record slaughter quality traits on whole dead and live fish using a medical CT scanner

5.2.1 Background

The aim of WP2 was two-fold: 1) to determine which traits can be measured in a CT scanner, and 2) for which of these traits it is possible to write automated software to allow efficient and standardised analysis of the CT images.

The removal of the intestines and head is achieved from a combination of locating anatomical landmarks and using deep learning algorithms. Algorithms have been implemented in a semiautomated software solution.

The aim was to determine, which quality traits that can be measured non-invasively to allow the measurement directly on the breeding candidates instead of the information collected in test-slaughter of sibs. Feasibility to use CT scanning for following traits was investigated and reported here:

- Fat in salmon
- Detection of Operational Welfare Indicators (OWI)
 - Emaciation
 - Upper jaw deformations
 - Lower jaw deformations
 - Exophthalmia
 - Operculum damage
 - Fin damage
 - Vertebral deformity
 - Detection of wounds
- Analysis of organs
 - Shape and size of the gonad
 - Shape and size of the heart
 - Size of the liver
- Prediction of pigmentation
- Estimation of melanin spots
- Gaping of the fillet

In general, the analysis given in this study suffers from a deficiency of phenotypic reference data as no complete data were provided for the different deformities. Validation whether particular features observed in CT scans are actual defects is difficult as no reference data was available.

5.2.2 Collection of data and scanning protocol

Data collection

Two sets of data were used for CT scanning. First, CT scans of dead fish were collected in connection of the test slaughter/manual dissection between 5th and 9th of March 2018 at Austevoll Laksepakkeri. The second dataset comprised CT scanning of live fish at Bremnes Seashore between 10th and 15th of November 2019. The data collection of the datasets is presented in Section **5.1.1**.

For the live fish scanning a total of 1,425 pre-selected SalmoBreed strain fish representing year-class 2018 were registered and CT scanned in connection of the ordinary test slaughter of full-sibs of the breeding nucleus (see also 5.1.2). Fish were sedated on a boat and their PIT-tag was scanned. Pre-selected, experimental fish were taken on land, allowed to recover from the first sedation, sedated for the second time (different sedative), CT scanned, and returned to recovery cage for a week's time before slaughter. Nets were used to carry and protect/calm down the fish during scanning. "Operational" time per fish was approximately 3.5 min from sedation to completed CT scanning. Total mortality in the connection of the recording was around 10 %.

Scanning

The scanning protocol for both operations was specifically optimized to enable scanning of 2,000 individuals in a 5-day period. The salmon were scanned three fish at a time in a custom-made fixture (Figure 6). The x-ray absorption properties of the fixture and PIT-tag and barcode were clarified. The fixture has low x-ray absorption, whereas PIT-tag can be easily separated from the surrounding tissues due to HU well above 2500. Barcode has the same density as the fins of the fish, but image analysis can be used to locate and segment the barcode if an absolute value of bone voxel for each salmon is needed. The following CT scanning parameters were used in the data collection:

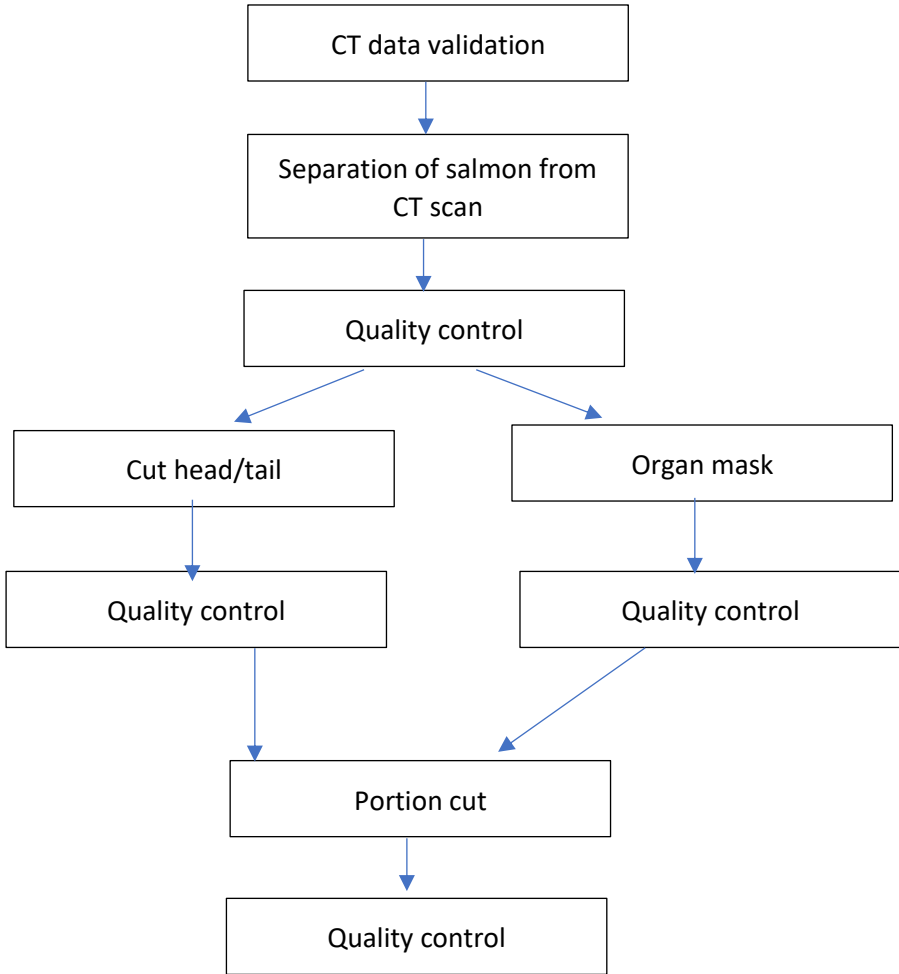
- 2 mm slice thickness, 2 mm slice distance
- Pixel spacing (0.781\0.781) mm
- Energy 100 kV
- Xray tube current 150 mA
- Exposure time 750 ms
- 112 mA exposure
- 40 cm field of view (L)
- Standard reconstruction (Toshiba FC01)

The full DICOM header is available in Appendix 2.



Figure 6 Fixture made in foam (Sundolitt). This type of fixture was used in CT scanning of dead fish and was further developed for the needs of live fish scanning.

Data process flow-chart



Cut head/tail

Cutting the head and tail of the salmon was preformed using feature engineering (Figure 7). The head was cut using two points; the two pectoral fins, the point where the spine and cranium meet the upper portion of the cut was made at a fixed angle to the spine.

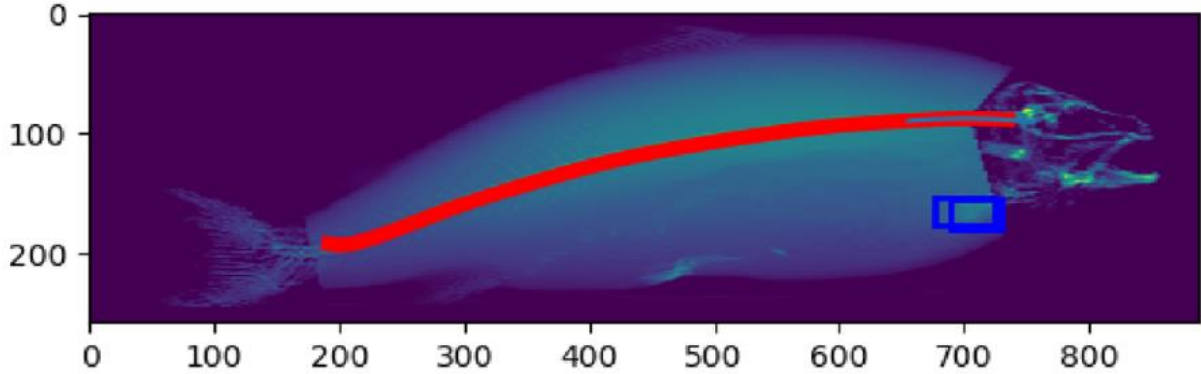


Figure 7 Validation image of the cut head/tail image.

Organ mask

An organ mask (Figure 8) was generated using a deep semantic segmentation network based on the Unet3D architecture. Fish were split into training and validation sets with a holdout of 20 test fish. Each fish was split in overlapping 32x32x32 pixel regions to allow them to fit in memory during training. Training was done solely on the regions. Model comparison used the full organ mask rebuild from the region based prediction. Final model selection compared the total pixel-wise accuracy and also the maximum deviation between the generated mask and the ground truth mask. This was also done in three regions in the axial orientation with the head region being the location of the major deviation with the other regions showing at most 2 pixel deviation between the generated mask and the ground truth. In the head region, the difference could be up to 7 pixels, and this is largely attributed to the higher variance of the region, this was also the region where the annotators were least sure of where to apply the mask and not.

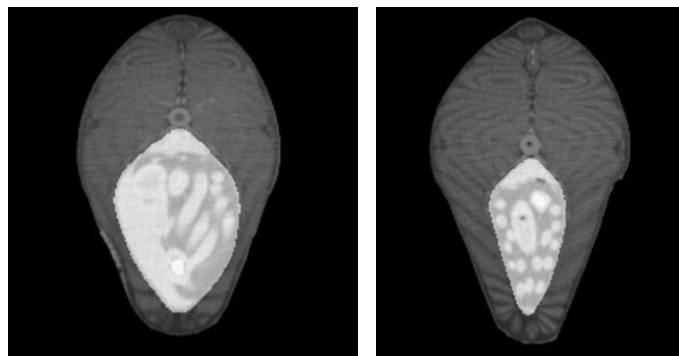


Figure 8 Organ masks.

Proportion cut

Cutting or separating the different parts and sides (left/right) of the salmon were performed using feature engineering. The left and right sides were separated using the spine and a constructed plain. The head and tail were found as previously described (cut head/tail section). The Norwegian quality cut (NQC) and the tail part was created from locating the caudal side of the dorsal fin and the cranial side of the anal fin. The tail finished with the beginning of the caudal fin (Figure 9). This dataset is referred to as proportion dataset in Section 5.4.2.

Extremely small salmon are in general difficult to handle and cut virtually as their small size reduces the relative resolution, and the portioning heavily relies on the location of certain fatty areas in absent in the smaller fish. We have not focused on optimizing the algorithm beyond a proof of concept.

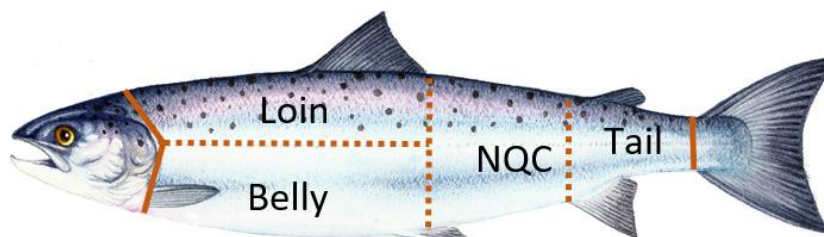


Figure 9 Proportion cut of salmon.

5.2.3 Fat in salmon

In this section, analysis of fat ratio and fat distribution is reported. Fat in the different parts of the salmon can be analysed using the same method. No reference/validation data on the amount of fat is directly correlated to the results in the given section.

Intramuscular fat

Intramuscular fat is quantified using image segmentation and spectral analysis. The intramuscular fat is defined as the fat in the muscle. To quantify this on the CT scan, several methods have been proposed:

- Otsu method
- The slope between the fat and meat part of the histogram
- The area of the density histogram related to the meat part

The **Otsu method** finds a separation point, a specific Hounsfield Unit value (HU) used to separate fat and meat in the CT scan (Figure 10). The Otsu method minimizes the inter-class-variation of the histogram.

The **slope** between the fat and meat is classified as the slope between the meat peak and the HU value at half peak (Figure 11, left panel). The better the separation of fat and meat, the steeper the slope and a hypothesis of less fat in the meat part.

The relative **meat-area** is another method used to quantify the amount of intramuscular fat in the fillet (Figure 11, right panel).

Otsu, differs between each fish, orange Fixed threshold, green=0

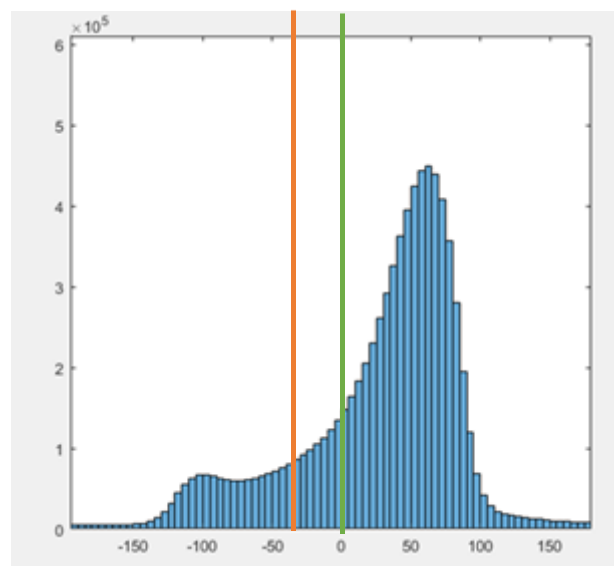


Figure 10 Illustration of the methods Otsu and Threshold.

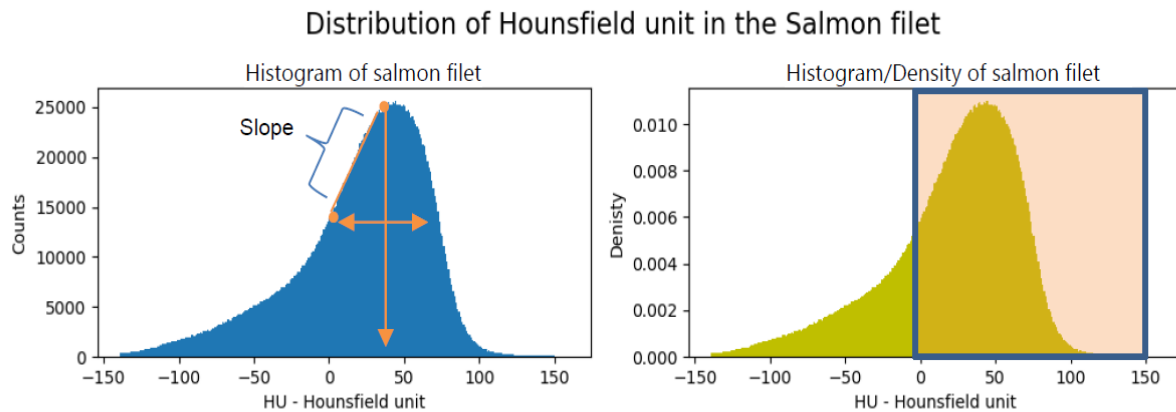


Figure 11 Methods of quantification of fat in the CT scan.

All the methods described above use the histogram of the salmon to quantify the intramuscular fat in the fillet. The higher the proportion of fat is in the muscle the wider will the shape of the meat part of the histogram be.

We can only make a hypothesis about the amount of intramuscular fat in the fillet. No independent measurement of intramuscular fat exists directly.

Example data

ID	fat	pigm	HWT	length	HU value at peak value	HU value at ½-peak	Meat area	Half to peak slope
6519	19.6	4.6	4600	66	52	12	79.2	378.5
6595	17.3	5.9	4340	64	62	23	83.9	393.6
6654	17	6.1	4680	64	56	16	79.3	395.7
6708	18.2	6.3	4780	69	56	7	77.3	298.8
6724	17.3	5	4500	66	56	16	80.8	386.9
6726	18.9	4.9	5020	70	59	10	77.3	328.7
6787	19.4	4.5	3980	61	40	-5	73.9	262.6
6821	18.4	5.9	4160	67	57	13	80.4	323.5
6839	19.6	4.7	3580	65	46	-2	74.3	228.7
6885	17.7	6.2	4120	66	55	16	81.5	356.1
7033	16.8	4.9	3400	62	56	13	80.2	251.3

Fat in fillet

The fat in the total salmon and in all the different parts, the masked sections (organ, head-on-gutted, fillet) can be analysed, and the amount of fat can be quantified.

An example of different amounts of fat is shown in Figure 12. Fat on the CT scan is darker compared to the more dens tissue (meat, bone), which are lighter in contrast (meat and bone).

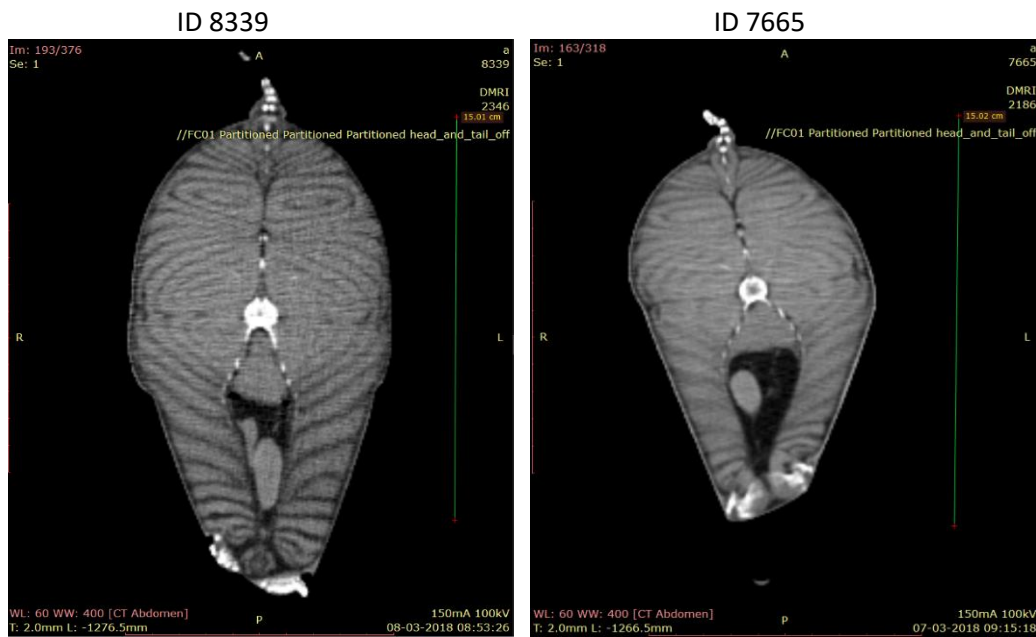


Figure 12 Examples of different amounts of fat in a cross sectional cut of CT scan.

5.2.4 Detection of OWI's

In this section, the possibility of detecting different **operational welfare indicators** (OWI) is discussed. The definition DMRI is currently working with, can be seen in <https://nofima.no/wp-content/uploads/2018/11/FISHWELL-OWI-poster-v1.1.pdf>. From the reference images given in the source, eye haemorrhaging, snout damage, skin haemorrhages, small lesions, scale loss and sea lice infections are detectable by CT. These are primarily colour variations and do not show consistent volumetric or density variations above the expected noise in the scan. Below we discuss which of the remaining OWI categories are detectable/undetectable using CT, and the analysis behind this investigation. The assessment of these features is hindered by the lack of reference data on which fish fall in which category. DMRI's assessment is on these indicators is descriptive due to the lack of this reference data.

Emaciation

Emaciation is a condition where the individual being exceptionally thin. Therefore, a comparison of external parameters is expected to be sufficient to identify emaciated fish. To illustrate this, we hypothesised that the relation of the total volume of the fish to its length, a low effort measurement, would prove that macro-parameters can be used to determine emaciation. No reference data on the presence or the degree of emaciation were available. Therefore, a qualitative study was conducted to examine the proportion of fish with an abnormal long "tube-like" body shape.

Comparing the group of fish with a low volume to length ratio with a random group in the middle of the distribution, the lower ratio group had a higher concentration of fish that appear emaciated.

Technically it is possible to extract number of parameters other than length and total volume, such as lean meat percentage, relative amount of fat in the gut, cross-sectional area and use these parameters to fit a linear model to the data. Linear model combined with reliable reference data would give a reliable method of identifying emaciated salmon.

Jaw deformity

Any jaw deformity is expected to originate from the structure of the bones in the upper or lower jaw. In the reference material, the upper jaw deformity was detectable in the shape of the upper head, usually as a shortened upper jaw relative to both the lower jaw and the length of the whole fish. The hypothesis was that upper jaw deformity could be detected by comparing the distance between the point where the spine is fixed to the head-atlas bone (triangle in Figure 13) and the tip of the snout (star in Figure 13) with the total length of the spine. These parameters can be extracted with a reliability above 95 % and therefore allow for a qualitative analysis of the data. The fish with the lowest ratio of these two distances had an upper jaw that was shorter than the lower jaw. No correlation was found between the ratio-phenotype described above and actual upper jaw deformity phenotype registered in the manual slaughter. Therefore, further investigation of these deformities may require a higher order analysis of the shape of the upper part of the head or more reference data.

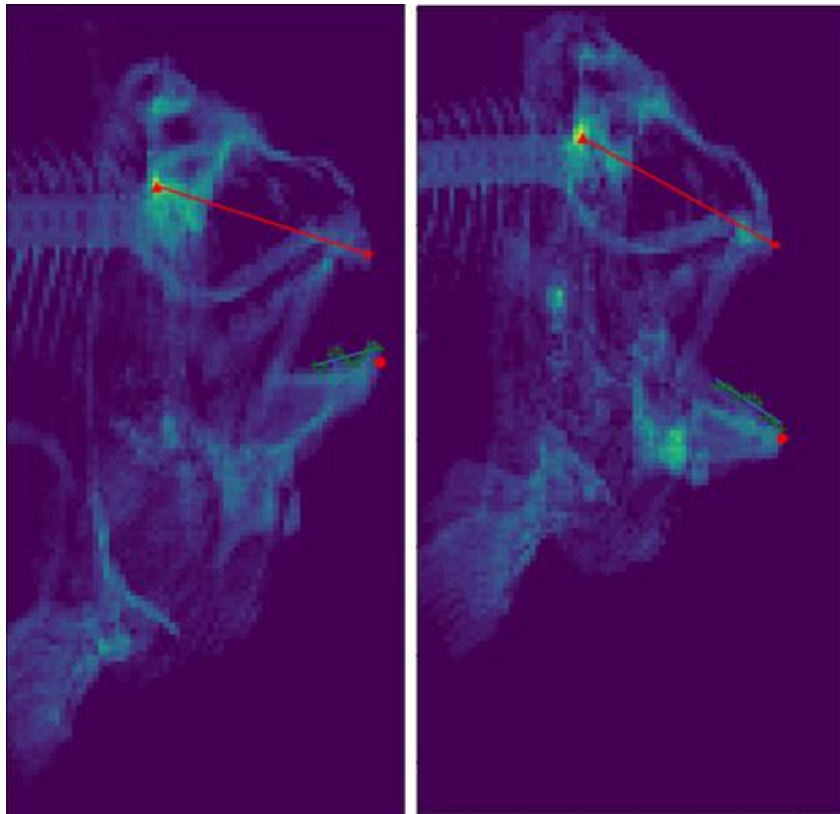


Figure 13 Two illustrations of the data extracted regarding the lower and upper jaw.

The lower jaw deformity is characterized by down curving and opening of the lower jaw. Our attempt of extracting number of descriptors from CT scans and coupling those with the manual slaughter phenotype showed that a reliable automated analysis of jaw deformities is unlikely to be successful. The cause of deformations to the jaw are not fully understood and due to the complexity of the deformity, a higher order shape analysis would be necessary.

Exophthalmia

The possibility to detect exophthalmia by CT scan was not investigated as this trait was not registered in the manual slaughter. Any automated system would most likely require a deep learning approach

as no reliable fixpoints are available to enable successful traditional image analysis. Following this, a model could be built to grade the eye based on its extrusion compared to the plane of the head.

Operculum deformity/damage

In the manual slaughter dataset, the cause (e.g., shortened operculum, damage due to handling) of the operculum damage was unknown. The fixture used during the CT scanning added distortion to the area where the operculum is located. Therefore, it stays uncertain whether the current protocol is suitable for detection of this deformity. This considering, side images were taken of all fish in the 2019 test slaughter. Manual inspection of these images allowed quick identification of the deformity; it is more relevant to develop a colour image-classification model for operculum damage than use CT scanning for detection of this trait.



Figure 14 Operculum damage during live fish scanning in November 2019. Easily identifiable damage enables grading based on photographs.

Fin damage

In this feasibility study, we investigated the possibility to detect fin damage on the dorsal fin from CT scans due to its high frequency, and because it is easy to isolate dorsal fin from its surrounding area (Figure 15). A first manual inspection of the dorsal fins on the CT image makes it clear that it is hard to determine with certainty that a fin is damaged, unless the damage is severe.

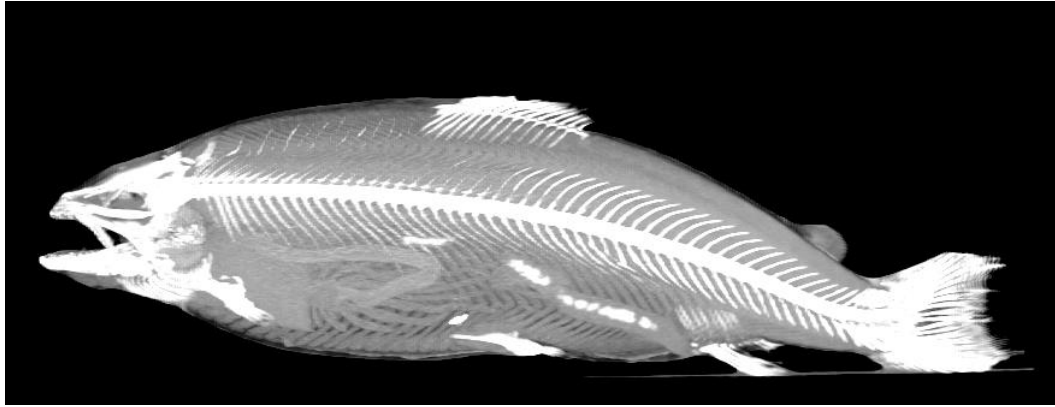


Figure 15 CT image to detect damage of inner and outer dorsal fin.

CT image of inner and outer dorsal fin

On the dorsal fin, several relative measures were extracted. This was done by defining an inner (under the skin) and an outer fin. When the fin is removed there is a natural surface of the back that can be recreated in the analysis. Any part of the fin outside this surface is defined as the outer fin, and fin bones inside the fish (defined by this surface) are considered the inner fins. Based on this distinction, the following parameters are extracted:

- Volume of outer fin
- Volume of bones in outer fin
- Volume of inner fin bones
- Volume of the meat in the outer fin (meat density)

The hypothesis was that damage to the outer fin is indicated as relative deviations from these quantities. Relative size of the outer and inner bones provided a measure with a high concentration of damaged fins in one end of the spectrum and none in the other end of the spectrum. This indicated that volumetric data contains relevant information to determine fin damage.

Number of shape parameters were extracted to improve the detection of fin damage: curvature, length, height and abrupt changes in the fin. A qualitative examination of these data showed that the extracted values were not unambiguous in fin damage detection.

Vertebral deformities

Grading of spinal deformities (see Figure 16) vary from fused vertebrae to the extremely deformed spine. We assessed whether severity categorisation would be possible using CT scans. A straightforward version would include the classification of deformities based on the projections of the spine as presented in Figure 17, since this presentation show the spine in the sagittal plan.

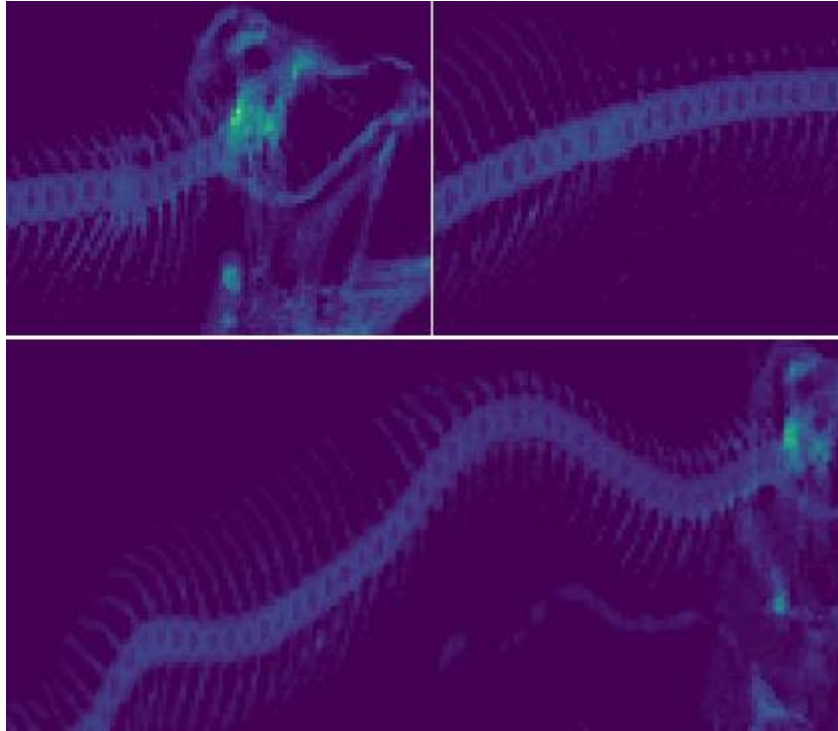


Figure 16 Examples of vertebral deformities. Upper left panel: likely a fracture, upper right panel: fusion of vertebrae, lower panel: severe spinal deformity (combination of lordosis and kyphosis).

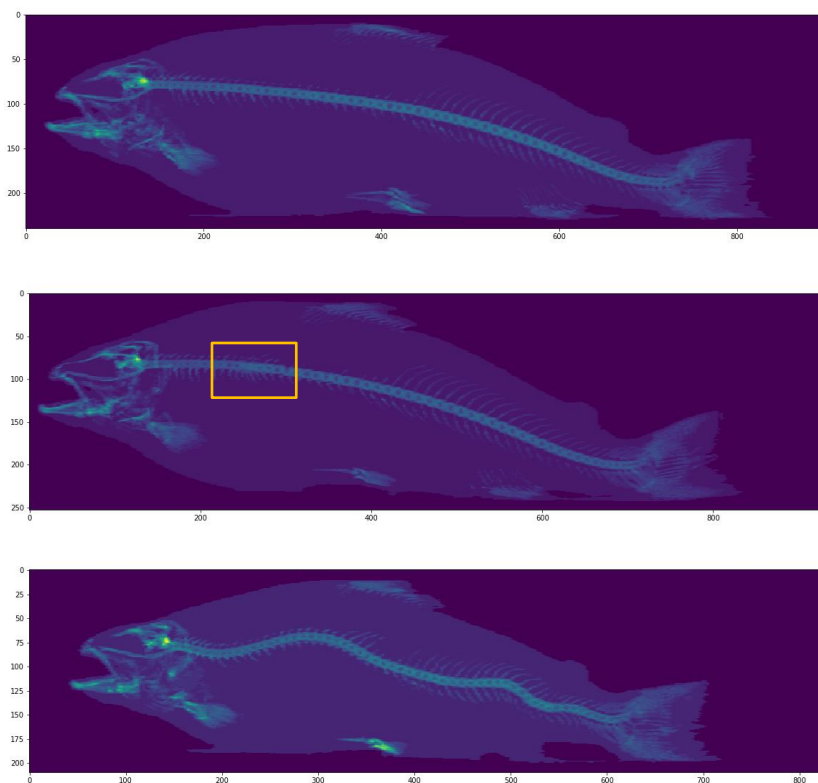


Figure 17 Upper panel: normal spine, mid panel: compressed vertebrae, bottom panel: severe spinal deformity.

Wounds

“Arnauds sår skala” (Appendix 1) was used for grading of salmon wounds in the manual slaughter. Figure 18 shows example of wounds detected on the salmon scanned in the 2018 test slaughter.

Large wounds can be detected in CT scan (Figure 18, left panel). However, a vision-based-system would be better suited for the application (Figure 18 right panel), as the wound is clearly visible in the photograph but barely visible in CT scan. The depression around the wound can be seen in the height profile of the fish and easily remains undetected due to noise and other variations in the data.

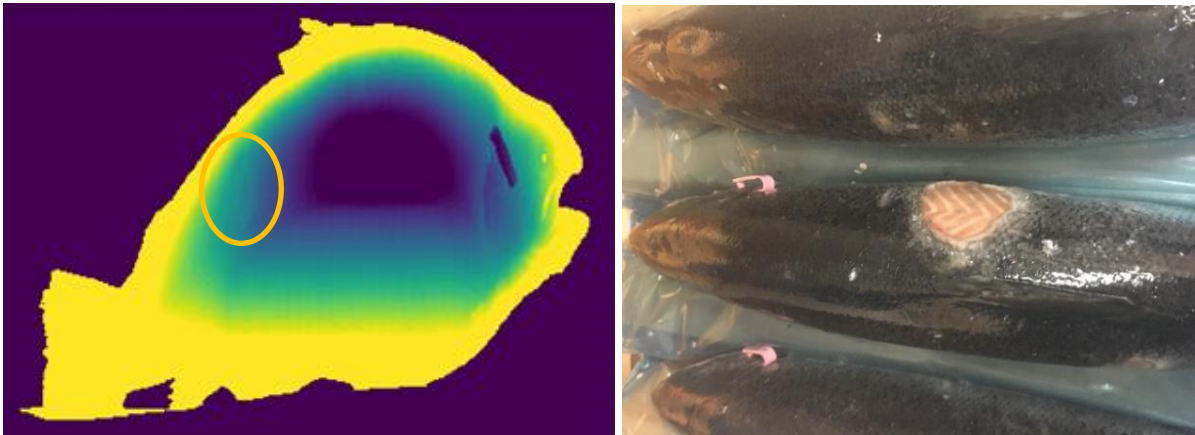


Figure 18 Example of severe wound observed in the test slaughter in 2018. Right panel shows the height profile of the fish, whereas on the right the actual wound is photographed.

5.2.5 Analysis of organs

The isolation of inner organs was done using deep learning where a model is trained to segment the organs following a segmentation of the intestines from the rest of the salmon. In principle, the method used here is the same as was used in the segmentation of the full intestinal region (organ mask, Figure 8). Here we only illustrate how the method works in organ analysis, and no attempt was made to refine the method over multiple iterations of training.

Shape and size of the gonads

Gonads between male and female salmon differ significantly (Figure 19). Therefore, any isolation algorithm developed for one would not be expected to work for the other. Having inspected a large quantity of CT scans, both the male and female gonads are easy to identify with minimal training.

In this study we only performed a segmentation of the female gonads as the size and shape of the female gonads is relevant to determine sexual maturity and the number of eggs they are expected to carry.

Once a deep learning model has been trained to isolate the gonads, it is a relative simple exercise to extract measurements such as absolute length, relative length as compared to the fish, cross-sectional area and volume to predict sexual maturity of the female fish.

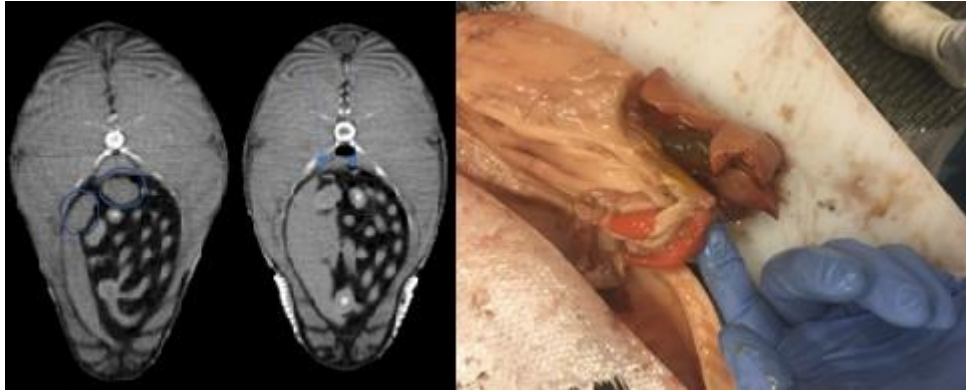


Figure 19 Location of the gonads if female and male salmon on the CT image (left panel), and actual gonads of gutted salmon (right panel).

Different deep learning networks were trained to locate and segment the gonads. The gonads are assumed to be located below the kidney, and therefore a region below the kidney is extracted, and in this region, the gonads were localised using deep learning (Figure 20).

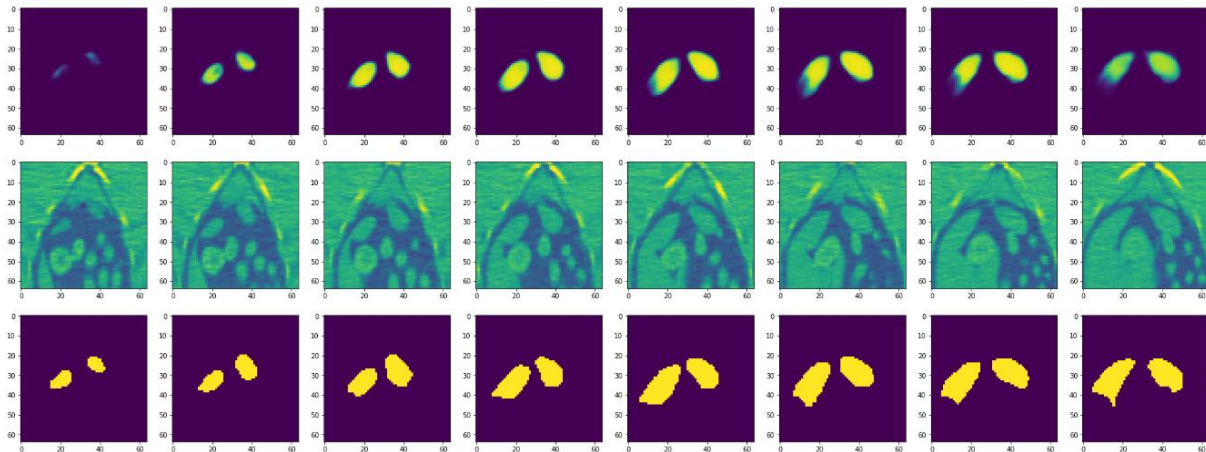


Figure 20 Top row: output from the deep learning algorithm, middle row: CT slice, bottom row: the annotated slice.

Shape and size of the heart

The shape and size of the heart was evaluated in as similar manner than the gonads, and isolated with the same algorithm. The absolute size of the heart is easy to extract, and more complex shape analysis can be performed if the heart is successfully segmented.

The heart is not well defined on the CT scans, and we did not have reference to validate the method. The model was trained on a manually annotated CT slice by DMRI staff with limited knowledge of salmon anatomy. As for the gonads, an approximate region was first extracted, and this region was then fed to the deep network for segmentation. As can be seen in Figure 21, the results offer a reasonable location of the heart.

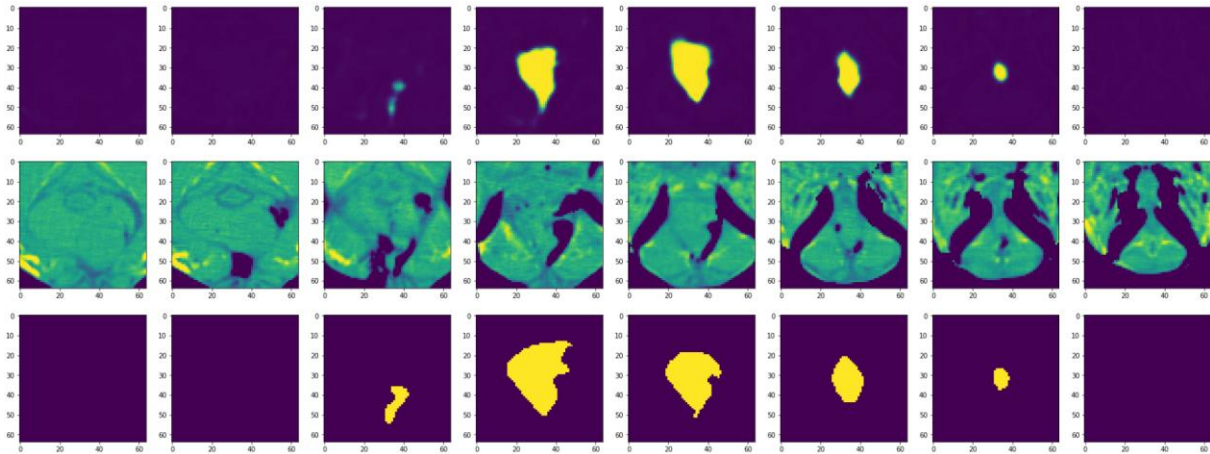


Figure 21 Top row: output from the deep learning algorithm, middle row: CT slice, bottom row: manually annotated heart. This is an example from one of the better segmentations.

Size of the liver

The size of the liver has been highlighted as a parameter of interest given that the algorithm can isolate the liver from the stomach and heart in a reliable way. It was relatively straightforward to extract size parameters for the liver to identify individuals with abnormally sized livers.

5.2.6 Pigmentation

Pigmentation of the fillet is important for the salmon industry from the economic and consumer acceptance point of view. Since this is based on visual colour it is highly unlikely to show up in the CT scan and it has not been possible to detect any indicators of this in our studies.

5.2.7 Melanin spots

Like pigmentation, the prerequisite for reliable detection of melanin spots would be significantly different density of spots from their surrounding areas, which was not observed.

5.2.8 Gaping

None of the fish used in this study had reliable gaping data available. Gaping is a phenomenon reliably observed post slaughter of fresh (not frozen) fish. In this project the salmon had either been frozen (Section 5.1.3. for details) or they were alive, and assessment of detecting gaping from CT scans was not feasible.

5.2.9 Conclusions for WP2

CT-scanning of large number of live individuals was successful and connected to acceptable operation time and low mortality.

Organ mask and proportion cuts of whole dead and live fish can be reliably be performed by CT scanning and segmentation methods presented here. Many of the traits of interest have relatively low frequency and therefore lead into an inadequate number of reference data for reliable method

validation (deformities). Additionally, some traits are more feasible to phenotype with high-throughput visual systems, such as outer deformities and wounding. One strength of this method is that novel post-scan phenotypes can be determined using the same CT scans and by adjusting the segmentation software.

The largest potential lies in using live fish CT scanning to provide precise phenotypes of high value cuts measured directly from breeding candidates. This allows minimizing the number of experimental animals and increased accuracy of the estimated breeding values, and given moderate heritabilities, increased genetic gain.

5.3 WP3: Measure pigmentation on whole, slaughtered fish

5.3.1 Background

Pigmentation is major quality feature of farmed salmon, but today there are no reported techniques that can be used to quantify pigmentation of salmon in whole or live fish. Recently, Nofima showed that a special type of Raman technique, namely spatially offset Raman spectroscopy (SORS), can be used to radiate through salmon skin and probe fatty acid and pigment features in muscle of whole salmon. In the present project, our aim was to evaluate the possibilities for quantitative analysis of pigmentation using Raman spectroscopy, and compare these findings with the state-of-the-art visible/near-infrared spectroscopy.

5.3.2 Pigmentation: dead fish

The first possibility for a comparative study of techniques for quantification of pigmentation in whole salmon came with the SalmoBreed manual slaughter spring 2018 (see **5.1.1**). For this test, three different analytical technologies for quantification of pigmentation was used: 1) The Qvision near-infrared scanner (for near-infrared analysis directly on fish fillets); 2) The Qpoint near-infrared measurement system (regularly used for live fish analysis of fat contents); and 3) A handheld SORS device (provided by Agilent).

Qvision

The Qvision near-infrared (NIR) scanner was used to scan approximately 5,600 salmon sides (fillet side) during the test slaughter (Figure 22). The existing calibrations of the scanner were used to predict fat and pigment contents of all measured salmon sides. All predictions were subsequently used in the genetic calculations (referred as FAT in section **5.4**). From the 5,600 samples, 30 were selected for reference analysis (the whole side was used in reference measurements of fat and pigments, respectively). Good correlations with feasible estimation errors were obtained for both parameters: Fat contents - RMSEP (Root mean square error of prediction): 0.6 % fat; and pigment contents – RMSEP: 0.6 mg / kg. This corresponds to previously reported results ((Heia, et al. 2016) and confirms that the Qvision NIR scanner performs well in these types of analysis.



Figure 22 Qvision measurement of salmon fillets during the first trial.

Qpoint

The Qpoint NIR measurement system was used to collect spectra of a total of 680 fish during the five-day manual slaughter. All measurements were performed on the skin side of the fish, on the ventral part above the anal fin. This sampling spot has earlier proved to be the most optimal spot for pigment analysis on whole salmon using NIR spectroscopy. From the 680 samples, reference analysis (i.e. pigment content in mg / kg) of 34 samples were provided. All reference analyses were performed on the Norwegian Quality Cut. The 34 reference samples showed a good range of variation (4.1 – 7.7 mg / kg). Partial Least-squares regression (PLSR) was used to establish a link between the Qpoint spectra and the corresponding pigment reference values. Only the “visible” part of the Qpoint spectra (i.e. 460 – 740 nm) was used in the regression. This is because the NIR region of the Qpoint spectra (i.e. 760 – 1040 nm) is known to carry no information on pigments.

The regression results showed that the correlation obtained was very poor ($R^2 = 0.2$), meaning that there is practically no link between the Qpoint spectra and the reference analysis. This can have number of reasons, including the following:

- We know from earlier experience that pigment quantification of whole fish using NIR is difficult, as the fish skin absorbs much of the visible light that is needed to detect the pigments.
- Reference analysis was done on NQC, i.e. not the same sampling spot as used for NIR measurements (the ventral part above the anal fin). Previous optimal results using NIR have been obtained when NIR analysis and reference sampling is done on the same spot.
- The results are based on a limited number of samples. Many people were involved in the fish trail, and several people handled the same samples. Thus, erroneous marking of a few of the samples would significantly affect results in such a limited data set.

SORS

The main aim of the measurements was to evaluate the potential of using spatially offset Raman spectroscopy to quantify pigments in salmon through the skin. Earlier studies at Nofima has shown that using one commercial system for SORS (the so-called RapID from Agilent), this could be feasible. Figure 23 provides a general schematic description of the optical configuration in question. In the conventional Raman backscattering configuration (left), Raman scattering excitation and detection is performed at the same sample position. For SORS (right), acquisition of Raman spectra is undertaken from regions spatially offset on the sample surface from the point of the excitation laser beam. Thus, with SORS, Raman collection is only done on photons that has travelled a given distance into the tissue.

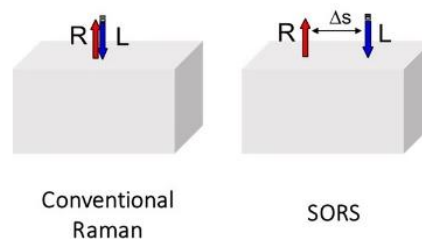


Figure 23 A general schematic description of the optical configuration of conventional Raman spectroscopy (left) and SORS (right), respectively.

The RapID can be characterized as a high-resolution instrument. The challenge for the project was that the time between project approval and the test slaughter was short, thus we were not able to borrow this RapID from Agilent. However, Agilent could provide us with a “simpler” system, a hand-held system called Resolve (Figure 24). This instrument arrived in Nofima a couple of days before the test slaughter, and initial testing of the instrument was performed in house.

All SORS measurements in the test slaughter were performed with a total accumulation time of 5 minutes per spectrum. The laser power of the instrument was fixed at 100 mW. The high spectral accumulation time was needed in order to achieve sufficient S/N ratios of the spectra. This is, however, a very long measurement time and not very practical in a test slaughter. In addition, since the instrument was hand-held during measurements, disturbances due to e.g., movement during measurement was bound to happen. All measurements were performed on the skin side of the fish, on the ventral part above the anal fin. A total of 236 salmon samples were measured with SORS during the test slaughter.



Figure 24 Measurement of pigmentation from whole dead fish with handheld SORS instrument.

A thorough review and interpretation of the obtained SORS-spectra revealed the following:

- The adipose tissue of sampled fish was clearly visible in the spectra, meaning that the photons involved in the measurement actually penetrate the skin and reach the adipose tissue beneath the skin.
- Concerning pigments, however, pigment bands are expected at intensities in the spectra fairly close to the general noise levels in the spectra. After close inspection of the spectra, no clear traces of pigments could be seen, meaning that with this SORS setup, the majority of the photons involved in the SORS measurement do not reach the actual salmon muscle where the pigments are present.

From the 239 samples, reference analysis (i.e. pigment content in mg / kg) of 31 samples were provided, coinciding with the samples described in chapter 5.3.2 above. All reference analyses were performed on the Norwegian Quality Cut. Partial Least-squares regression (PLSR) was used to establish a link between the SORS spectra and the corresponding pigment reference values. The regression results showed that the correlation obtained was very poor ($R^2 = 0.3$), meaning that there is practically no link between the SORS spectra and the reference analysis.

5.3.3 Discussion and conclusions on pigmentation measurements, dead fish

The following conclusions were drawn from the initial experiment of the project:

- NIR scanning of salmon muscle sides is expectedly robust for quantification of fat and pigments.
- The Qpoint NIR system did not provide robust models for quantification of pigments in whole fish. These results confirm earlier studies showing that the visible light used in the measurements (which is needed for pigment quantification) is absorbed by the skin. If the Qpoint approach is going to be used for live fish trails in 2019, an improved sampling regime is needed. This is expected to improve prediction accuracies.

- The instrument settings of the hand-held SORS approach used in the study (i.e. the Resolve instrument) do not allow quantitative information of the pigments in whole salmon to be obtained. Only lipid information from the adipose tissue beneath the skin could be obtained. In addition, the time needed to perform the SORS analysis, was too long for practical use in fish trails. Nofima has earlier shown that a high-resolution SORS system (i.e. the RapID from Agilent) could be used to get semi-quantitative information on pigments in whole salmon, in a time frame that is suitable for live fish analysis (1-2 minutes). The natural next step in the project is thus rental of such a system spring 2019 to establish the feasibilities for live fish analysis using RapID.

Based on the experience from the test slaughter, the following conclusions on technology for analysis of pigments could be drawn:

- The Qvision near-infrared scanner is a feasible reference tool for rapid scanning of pigments in salmon fillets. It was thus decided that this tool was used for pigment analysis in the subsequent part of the project.
- The Qpoint analysis of whole fish was not satisfying, and it was thus decided that this tool should not be part of the subsequent live fish trail.
- The handheld SORS device from Agilent did not provide enough resolution and laser power to penetrate deep enough into the salmon tissue. For the subsequent part of the project, it was thus to employ the RapID system from Agilent, which is a higher resolution instrument.

Throughout the project, frequent contact was made between Agilent and Nofima in order to rent a RapID system for the live fish trail autumn 2019. However, as it turned out, rental of such a system was not possible. Meanwhile, new studies at Nofima with a conventional Raman system (so-called Phat-probe system for Kaiser optical solutions), showed that deep penetration in muscle tissues using conventional Raman spectroscopy can also be achieved. The Phat-probe system was originally developed for representative tablet measurements (pharmaceutical industry), but the system is now also studied for applications on heterogeneous food matrices. What was seen in Nofima, was that while measuring salmon fillets (with skin) on plastic trays, clear fingerprints of the plastic trays were seen. This means that the photons actually penetrate the salmon skin. Thus, studies were performed on the Phat-probe system for understanding penetration depths in model systems and salmon muscle, with and without skin. These results were compared with similar results obtained on the RapID SORS system (in other projects). The main conclusions from these studies, is that for penetration in salmon tissue and other types of adipose tissue, the penetration depths of the Phat probe and the RapID SORS probe is similar (around 1 cm depth penetration could be achieved). However, when the muscle is measured through salmon skin, the pigment information from the salmon is only seen when using the RapID system. For the Phat-probe system, the reason why plastic can be “seen” through the skin, but not pigments, is most likely related to different Raman scattering efficiencies of the two materials, i.e. pigments have far lower scattering efficiencies than plastics.

5.3.4 Pigmentation: live fish

For the live fish trail autumn 2019, approximately 400 fillets were sent to Nofima for routine VIS/NIR analysis of fat and pigmentation (i.e. Qvision scanner, see section 5.1.1). Out of these samples, 30 extremes were chosen for chemical analysis and measured with the conventional Raman instrument in-house. The results are reviewed above. In addition, the same samples have been shipped to

Australia to a new collaboration partner at the RMIT University (in Melbourne, Australia) doing research using the RapID system. The partners are currently working on a joint publication comprising these and previously obtained results using the RapID SORS system and the Phat-probe system for analysis of pigmentation in whole salmon. Due to the Covid-19 lock-down in Australia, the University labs have been closed. Thus, we are still waiting to finalise the results.

5.4 WP4: Estimation of genetic parameters and genome wide association study

5.4.1 Genetic parameters for production and fillet quality traits from manual slaughter

Trait abbreviations and definitions are presented in Table 1.

Following univariate model was fitted to estimate genetic parameters for all production and fillet quality traits from manual slaughter:

$$\mathbf{y} = \mathbf{X}\mathbf{b} + \mathbf{Z}_A\mathbf{a} + \mathbf{Z}_C\mathbf{c} + \mathbf{e},$$

where, \mathbf{y} is the vector of the phenotypic observations ; \mathbf{b} is the vector of fixed effect of sex (male and female; fitted for HWT, LGTH, GWT, FWT, FYGWT, FYHWT, FAT, PIGM, WND, and TWS), of fat (fitted for GAP, MeISc and PMel), and overall mean (fitted for FDef); \mathbf{a} is the vector of random additive genetic effects; \mathbf{c} is the vector of random family effect (accounting for maternal and effect of common environment shared among the full-sibs before communal rearing) and this effect was dropped from the model for traits that showed no significant family effect: PIGM, WND, TWS, GAP, MeISc, PMel and FDef; \mathbf{e} is the vector of random residual effects. The \mathbf{X} , \mathbf{Z}_A and \mathbf{Z}_C are the design matrices assigning observations to the levels of fixed effect, additive genetic effects, and family effects, respectively.

Genetic parameters were estimated using ASReml (Gilmour et al. 2009). Bivariate or multivariate analysis of ASReml allow only inclusion of one binary trait. Thus, to enable bivariate and multivariate analysis, WND and PMel were analysed in observed scale using linear model. If the binary score in the original data is evenly distributed, that is 50-50, linear and threshold models are expected to result in similar results. This was confirmed by the univariate analysis, the heritabilities for WND in linear and threshold models (using sire-dam model) were similar, 0.031 ± 0.022 and 0.021 ± 0.015 , respectively. While, for PMel, the heritabilities were 0.042 ± 0.031 and 0.025 ± 0.019 , for linear and threshold models, respectively. For the FDef, the ratio between “0” and “1” was 0.9:0.1, thus, this trait did not comply the assumption and was analysed in probit scale using the binomial option in ASReml. The results from univariate analysis for FDef was analysed by sire-dam model.

Genetic correlations between the traits were estimated with multivariate animal model. Bivariate analysis was first carried out to provide starting values (the variance-covariance matrices for residual and genetic structures) in ASReml analysis. The 4-trait multivariate model in matrix form was as follows:

$$\begin{bmatrix} \mathbf{y}_1 \\ \mathbf{y}_2 \\ \mathbf{y}_3 \\ \mathbf{y}_4 \end{bmatrix} = \begin{bmatrix} \mathbf{X}_1 & 0 & 0 & 0 \\ 0 & \mathbf{X}_2 & 0 & 0 \\ 0 & 0 & \mathbf{X}_3 & 0 \\ 0 & 0 & 0 & \mathbf{X}_4 \end{bmatrix} \begin{bmatrix} \mathbf{b}_1 \\ \mathbf{b}_2 \\ \mathbf{b}_3 \\ \mathbf{b}_4 \end{bmatrix} + \begin{bmatrix} \mathbf{Z}_{1A} & 0 & 0 & 0 \\ 0 & \mathbf{Z}_{2A} & 0 & 0 \\ 0 & 0 & \mathbf{Z}_{3A} & 0 \\ 0 & 0 & 0 & \mathbf{Z}_{4A} \end{bmatrix} \begin{bmatrix} \mathbf{a}_1 \\ \mathbf{a}_2 \\ \mathbf{a}_3 \\ \mathbf{a}_4 \end{bmatrix} + \begin{bmatrix} \mathbf{Z}_{1C} & 0 & 0 & 0 \\ 0 & \mathbf{Z}_{2C} & 0 & 0 \\ 0 & 0 & \mathbf{Z}_{3C} & 0 \\ 0 & 0 & 0 & \mathbf{Z}_{4C} \end{bmatrix} \begin{bmatrix} \mathbf{c}_1 \\ \mathbf{c}_2 \\ \mathbf{c}_3 \\ \mathbf{c}_4 \end{bmatrix} + \begin{bmatrix} \mathbf{e}_1 \\ \mathbf{e}_2 \\ \mathbf{e}_3 \\ \mathbf{e}_4 \end{bmatrix},$$

where, subscripts 1, 2, 3 and 4 refer to variables 1, 2, 3 and 4. The rest of the notations are the same as mentioned above. Attempts to analyse all the 14 traits simultaneously (or as many of them as possible) failed due to the correlation structure between the traits; some of the traits are highly correlated resulting in convergence and/or singularity problems. Consequently, a 4-trait model was the largest that could be fitted on this data set.

Note that no family effect was fitted to PIGM, WND, TWS, GAP, MeISc, PMel and FDef in bivariate and multivariate models. To obtain the complete set of correlations between all 14 traits, 34 four-trait runs were performed. For each of 4-trait run, two different sub-models were performed, i.e. with inclusion (submodel 1) or exclusion (submodel 2) of family effect in the model. Although univariate analysis had indicated significance of family effect for some of the traits, the inclusion of family effect in multivariate model resulted in issue that the family variances could not be properly estimated, i.e. even though the model is converged, these variance were liable to change from positive definite to fixed at boundary. This could be due to traits were highly correlated and/or the data is not large enough to have the family effect well estimated.

The phenotypic and genetic parameters estimated from univariate and multivariate are presented in Table 6, and genetic and phenotypic correlations are presented in Tables 7 and 8. Due to trait combinations (in total 34) in multivariate analysis to cover the whole correlation structure, each trait was analysed multiple times resulting in several estimates of the same parameters. Thus, the estimates from multivariate models presented in Tables 6, 7, and 7 are averaged across the multivariate runs.

Estimates of heritabilities and family effect

Mean of the estimates of heritability (h^2) and family effect (c^2) from univariate and multivariate analysis (with family effects) were relatively similar (Table 6). Estimates of c^2 were low and varied between 4 and 6 percent for all traits except for both fillet yield traits, which expressed higher proportion of family variation: 13 % and 14 % for FYGWT and FYHWT, respectively.

In this study, the h^2 for both MeISc and PMel were 0.011 ± 0.016 and 0.025 ± 0.019 (univariate model, Table 6). These estimates indicate only low genetic variation for melanin and additionally the heritability estimates were coupled with high standard errors. More data may be needed for traits with such low heritability to enable good estimates.

Note that the estimates for FDef (mean h^2 of 0.15 ± 0.06) were obtained from sire-dam model, as sire-dam is preferable when threshold model is used. Additionally, animal model using probit scale and binomial option in ASReml was run. The heritability estimate from animal model was 0.099 ± 0.043 . Based on the comparison, sire-dam model has given slightly larger estimate of heritability.

Table 6 Phenotypic and genetic parameters for production and fillet quality traits from univariate, multivariate with and without random family effect.

Variables	Parameter	Model		
		Univariate	Multivariate: Submodel 1 ^a	Multivariate: Submodel 2 ^a
HWT	σ_A^2 (s.e.)	148683.000 (48908.900)	154178.000 (48562.800)	272037.900 (38134.030)
	σ_C^2 (s.e.)	40336.600 (17237.900)	40698.300 (17059.500)	-
	σ_P^2 (s.e.)	635400.600 (20895.00)	643604.100 (21074.900)	665794.400 (22639.900)
	h^2 (s.e.)	0.234 (0.073)	0.240 (0.071)	0.409 (0.047)
	c^2 (s.e.)	0.064 (0.028)	0.063 (0.027)	-
LGTH	σ_A^2 (s.e.)	4.455 (1.266)	4.510 (1.270)	6.633 (0.950)
	σ_C^2 (s.e.)	0.711 (0.419)	0.740 (0.418)	-
	σ_P^2 (s.e.)	16.897 (0.554)	16.953 (0.556)	17.353 (0.529)
	h^2 (s.e.)	0.264 (0.070)	0.266 (0.070)	0.382 (0.046)
	c^2 (s.e.)	0.042 (0.025)	0.045 (0.025)	-
GWT	σ_A^2 (s.e.)	142096.000 (42165.000)	1333495.000 (40177.600)	216536.000 (30014.200)
	σ_C^2 (s.e.)	24038.400 (13815.200)	27842.400 (13495.700)	-
	σ_P^2 (s.e.)	500697.400 (17248.000)	500477.600 (16803.100)	516674.200 (17732.600)
	h^2 (s.e.)	0.284 (0.079)	0.267 (0.075)	0.419 (0.048)
	c^2 (s.e.)	0.048 (0.028)	0.056 (0.027)	-
FWT	σ_A^2 (s.e.)	66541.100 (20664.900)	63710.900 (19754.900)	107696.900 (14838.000)
	σ_C^2 (s.e.)	13235.100 (6857.560)	14260.900 (6691.300)	-
	σ_P^2 (s.e.)	237671.200 (8281.000)	237679.000 (8139.300)	246514.300 (8676.400)
	h^2 (s.e.)	0.280 (0.081)	0.268 (0.078)	0.437 (0.049)
	c^2 (s.e.)	0.056 (0.029)	0.060 (0.029)	-
FYGWT	σ_A^2 (s.e.)	3.566 (1.792)	3.407 (1.747)	14.221 (1.865)
	σ_C^2 (s.e.)	3.233 (0.790)	3.372 (0.788)	-
	σ_P^2 (s.e.)	24.809 (0.816)	25.523 (0.832)	27.772 (1.054)
	h^2 (s.e.)	0.144 (0.070)	0.133 (0.067)	0.512 (0.052)
	c^2 (s.e.)	0.130 (0.032)	0.132 (0.031)	-
FYHWT	σ_A^2 (s.e.)	2.695 (1.531)	2.573 (1.478)	12.756 (2.681)
	σ_C^2 (s.e.)	3.146 (0.717)	3.230 (0.708)	-
	σ_P^2 (s.e.)	22.645 (0.731)	22.794 (0.731)	24.851 (0.942)
	h^2 (s.e.)	0.119 (0.066)	0.113 (0.064)	0.513 (0.052)
	c^2 (s.e.)	0.139 (0.031)	0.142 (0.030)	-
FAT	σ_A^2 (s.e.)	1.594 (0.414)	1.450 (0.385)	2.305 (0.303)
	σ_C^2 (s.e.)	0.189 (0.128)	0.236 (0.126)	-
	σ_P^2 (s.e.)	4.726 (0.170)	4.693 (0.163)	4.898 (0.177)
	h^2 (s.e.)	0.337 (0.080)	0.309 (0.076)	0.471 (0.046)

	c^2 (s.e.)	0.040 (0.028)	0.050 (0.027)	-
PIGM^b	σ_A^2 (s.e.)	0.375 (0.047)	0.380 (0.048)	0.377 (0.047)
	σ_P^2 (s.e.)	0.694 (0.027)	0.696 (0.027)	0.693 (0.027)
	h^2 (s.e.)	0.540 (0.052)	0.546 (0.052)	0.545 (0.053)
WND^c	σ_A^2 (s.e.)	0.005 (0.004)	0.005 (0.004)	0.005 (0.004)
	σ_P^2 (s.e.)	0.248 (0.006)	0.248 (0.006)	0.248 (0.006)
	h^2 (s.e.)	0.021 (0.015)	0.021 (0.015)	0.021 (0.015)
TWS	σ_A^2 (s.e.)	0.014 (0.009)	0.014 (0.009)	0.014 (0.009)
	σ_P^2 (s.e.)	0.575 (0.015)	0.575 (0.015)	0.575 (0.015)
	h^2 (s.e.)	0.024 (0.016)	0.024 (0.016)	0.024 (0.015)
GAP	σ_A^2 (s.e.)	0.928 (0.239)	1.052 (0.268)	1.105 (0.265)
	σ_P^2 (s.e.)	6.790 (0.225)	6.913 (0.234)	6.971 (0.240)
	h^2 (s.e.)	0.137 (0.034)	0.152 (0.037)	0.171 (0.039)
MeISc (Transformed by log (1+x))	σ_A^2 (s.e.)	0.003 (0.004)	0.004 (0.004)	0.004 (0.004)
	σ_P^2 (s.e.)	0.235 (0.007)	0.236 (0.008)	0.236 (0.008)
	h^2 (s.e.)	0.011 (0.016)	0.016 (0.02)	0.015 (0.016)
PMel^f	σ_A^2 (s.e.)	0.005 (0.004)	0.006 (0.004)	0.006 (0.004)
	σ_P^2 (s.e.)	0.216 (0.007)	0.217 (0.007)	0.217 (0.007)
	h^2 (s.e.)	0.025 (0.019)	0.030 (0.020)	0.029 (0.019)
FDef^d	σ_A^2 (s.e.)	0.163 (0.070)	0.166 (0.070)	0.166 (0.071)
	σ_P^2 (s.e.)	1.082 (0.035)	1.083 (0.035)	1.083 (0.035)
	h^2 (s.e.)	0.151 (0.060)	0.153 (0.060)	0.153 (0.060)

^a Estimates presented were average across different multivariate models.

^b Model with random family effect was run; likelihood ratio test between full and reduced models was, $\chi^2_{1df} = 0.48$, $p = 0.49$, which indicated that inclusion of random family effect did not significantly improve the model. Heritability reduced to 0.484 ± 0.093 with the inclusion of random family effect.

^c WND and PMel were both analyzed under observed scale.

^d FDef was analyzed under liability scale.

Phenotypic and genetic correlations

Trait combinations of TWS and WND, and MeISc and PMel, were highly genetically correlated. Adding a third trait in the multivariate analysis with these highly correlated traits resulted in convergence problems; correlations for these traits are estimates from bivariate analysis (Table 7).

The phenotypic correlations presented in Table 7 are estimates averaged across different multivariate runs. The estimates from models with family effects are presented at the upper diagonal and without family effects at the lower diagonal. Overall, the difference between estimates from models with and without family effects were relatively small, except those estimates in red fonts (Table 7). Note that family effect was fitted only for the traits where family effect was significant in univariate analysis. The highly correlated traits, in terms of the phenotype, were HWT, LGTH, GWT and FWT (Table 7); phenotypic correlations ranged from 0.80 to 0.99 for both with and without family effects. With no surprise, FYGWT and FHWWT were also highly phenotypically correlated. The rest of the traits were not phenotypically correlated with each other.

Table 8 shows the genetic correlations between the traits from models with (upper diagonal) and without family effects (lower diagonal). The differences between correlations from models with and without family effects were relatively large, for example, HWT and FYGWT had correlated of 0.283

from model with family effect and 0.0640 from model without family. This could be due to the exclusion of family effects from the models, which changed the estimate of covariances. Even though the differences were large, most of the correlations were still at the same sign, except those correlations in red fonts (Table 8), which has changed from negative to positive or *vice versa*. Same as their phenotypic correlations, HWT, LGTH, GWT and FWT were genetically highly correlated. Again, FYGWT and FYHWT were basically the same trait, genetically. Note that the genetic correlations between both melanin traits (MeIsc and PMel) and body measurement traits (HWT, LGTH, GWT and FWT) were relatively high and negatively correlated (Table 8), which means the larger the fish, the smaller the melanin score or least chance of presence of melanin on their fillet. However, the standard errors for all these correlations were relatively large (most were at least 50 % of their estimates). Further investigation is indeed needed to verify the results. Both melanin traits were also highly and negatively correlated with pigment (Table 8).

Table 7 Phenotypic correlations (s.e.) between different production and fillet quality traits for multivariate models with (upper diagonal) and without random family effects (lower diagonal). Correlations presented are averaged over different multivariate runs.

Trait	HWT	LGTH	GWT	FWT	FYGWT	FYHWT	FAT	PIGMT	WND	WSV	GAP	MelSc	Mel	FDef
HWT		0.873 (0.005)	0.988 (0.001)	0.908 (0.004)	0.127 (0.023)	0.120 (0.023)	0.376 (0.021)	0.229 (0.024)	-0.022 (0.019)	-0.050 (0.019)	-0.040 (0.026)	-0.050 (0.023)	-0.054 (0.024)	-0.036 (0.027)
LGTH	0.874 (0.005)		0.884 (0.009)	0.800 (0.008)	0.089 (0.023)	0.140 (0.022)	0.271 (0.023)	0.218 (0.024)	-0.014 (0.019)	-0.027 (0.019)	-0.079 (0.026)	-0.060 (0.023)	-0.064 (0.024)	-0.118 (0.027)
GWT	0.988 (0.001)	0.885 (0.005)		0.924 (0.003)	0.136 (0.023)	0.179 (0.022)	0.388 (0.021)	0.232 (0.024)	-0.027 (0.019)	-0.058 (0.019)	-0.037 (0.026)	-0.061 (0.024)	-0.065 (0.024)	-0.038 (0.028)
FWT	0.903 (0.005)	0.800 (0.009)	0.921 (0.004)		0.493 (0.018)	0.512 (0.017)	0.415 (0.020)	0.2300 (0.025)	-0.026 (0.019)	-0.057 (0.019)	-0.084 (0.026)	-0.057 (0.024)	-0.061 (0.024)	-0.047 (0.028)
FYGWT	0.116 (0.025)	0.086 (0.025)	0.131 (0.025)	0.499 (0.019)		0.939 (0.003)	0.219 (0.023)	0.089 (0.026)	-0.001 (0.019)	0.017 (0.019)	-0.150 (0.027)	-0.006 (0.024)	-0.001 (0.024)	-0.013 (0.027)
FYHWT	0.110 (0.025)	0.135 (0.025)	0.168 (0.025)	0.515 (0.019)	0.944 (0.003)		0.234 (0.022)	0.092 (0.026)	-0.019 (0.019)	-0.038 (0.019)	-0.159 (0.027)	-0.023 (0.024)	-0.018 (0.024)	-0.013 (0.027)
FAT	0.371 (0.021)	0.275 (0.023)	0.384 (0.021)	0.430 (0.020)	0.265 (0.024)	0.278 (0.024)		0.115 (0.026)	-0.004 (0.019)	-0.001 (0.019)	0.213 (0.025)	-0.077 (0.024)	-0.087 (0.024)	0.049 (0.028)
PIGMT	0.208 (0.025)	0.203 (0.024)	0.211 (0.025)	0.212 (0.026)	0.079 (0.027)	0.084 (0.027)	0.104 (0.026)		-	-	-	-	-	-
WND	-0.024 (0.019)	-0.014 (0.019)	-0.029 (0.019)	-0.022 (0.019)	0.010 (0.020)	-0.007 (0.020)	0.003 (0.0200)	0.059 (0.019)		-	-	-	-	-
WSV	-0.050 (0.019)	-0.026 (0.019)	-0.057 (0.019)	-0.051 (0.020)	-0.006 (0.020)	-0.027 (0.020)	0.007 (0.0200)	0.057 (0.019)	0.898 (0.004) ^a		-	-	-	-
GAP	-0.041 (0.027)	-0.081 (0.026)	-0.045 (0.027)	-0.110 (0.027)	-0.205 (0.029)	-0.214 (0.028)	0.173 (0.027)	-0.003 (0.026)	-0.029 (0.022)	-0.031 (0.023)		-	-	-
MelSc	-0.053 (0.024)	-0.064 (0.023)	-0.064 (0.024)	-0.055 (0.024)	0.003 (0.026)	-0.013 (0.026)	-0.071 (0.025)	-0.067 (0.023)	0.032 (0.022)	0.044 (0.022)	0.032 (0.022)		-	-
PMel	-0.054 (0.024)	-0.066 (0.024)	-0.065 (0.024)	-0.059 (0.025)	0.006 (0.026)	-0.012 (0.026)	-0.082 (0.025)	-0.074 (0.023)	0.019 (0.022)	0.029 (0.022)	0.021 (0.023)	0.923 (0.003) ^a		-
FDef	-0.035 (0.029)	-0.113 (0.028)	-0.036 (0.029)	-0.038 (0.031)	-0.009 (0.036)	-0.005 (0.036)	0.053 (0.032)	-0.008 (0.031)	-0.025 (0.020)	-0.039 (0.020)	0.087 (0.023)	0.014 (0.020)	0.019 (0.021)	

^a Estimates from bivariate models.

Table 8 Genetic correlations (s.e.) between different production and fillet quality traits for multivariate models with (upper diagonal) and without random family effects (lower diagonal). Correlations presented were average across different multivariate models.

Trait	HWT	LGTH	GWT	FWT	FYGWT	FYHWT	FAT	PIGMT	WND	WSV	GAP	MelSc	Mel	FDef
HWT		0.927 (0.0333)	0.999 (0.002)	0.963 (0.025)	0.283 (0.268)	0.489 (0.299)	0.447 (0.168)	0.287 (0.132)	0.136 (0.281)	0.226 (0.270)	0.168 (0.189)	-0.847 (0.441)	-0.630 (0.275)	0.272 (0.230)
LGTH	0.916 (0.018)		0.918 (0.034)	0.838 (0.065)	0.105 (0.250)	0.244 (0.296)	0.206 (0.179)	0.296 (0.119)	0.098 (0.271)	0.131 (0.260)	-0.077 (0.172)	-0.834 (0.417)	-0.641 (0.259)	0.134 (0.226)
GWT	0.988 (0.003)	0.926 (0.016)		0.965 (0.021)	0.227 (0.258)	0.498 (0.287)	0.463 (0.161)	0.295 (0.128)	0.149 (0.276)	0.217 (0.267)	0.149 (0.177)	-0.851 (0.436)	-0.643 (0.269)	0.308 (0.224)
FWT	0.890 (0.020)	0.829 (0.032)	0.910 (0.017)		0.411 (0.234)	0.5709 (0.212)	0.521 (0.152)	0.160 (0.122)	0.146 (0.275)	0.246 (0.259)	-0.019 (0.178)	-0.778 (0.436)	-0.614 (0.287)	0.268 (0.232)
FYGWT	0.064 (0.096)	0.059 (0.097)	0.111 (0.095)	0.514 (0.070)		0.960 (0.030)	0.555 (0.201)	-0.251 (0.174)	0.208 (0.379)	0.393 (0.355)	-0.454 (0.193)	0.063 (0.548)	-0.047 (0.447)	0.109 (0.375)
FYHWT	0.099 (0.096)	0.113 (0.097)	0.145 (0.094)	0.544 (0.068)	0.989 (0.003)		0.632 (0.206)	-0.144 (0.171)	0.267 (0.381)	0.366 (0.365)	-0.520 (0.180)	-0.010 (0.536)	-0.136 (0.442)	0.318 (0.373)
FAT	0.353 (0.086)	0.286 (0.091)	0.398 (0.082)	0.636 (0.061)	0.735 (0.053)	0.765 (0.050)		0.157 (0.109)	0.119 (0.258)	0.138 (0.242)	0.239 (0.165)	-0.174 (0.367)	-0.187 (0.281)	0.393 (0.216)
PIGMT	0.120 (0.092)	0.172 (0.092)	0.138 (0.091)	0.062 (0.092)	-0.136 (0.090)	-0.080 (0.091)	0.090 (0.090)		-	-	-	-	-	-
WND	0.066 (0.247)	0.091 (0.245)	0.092 (0.245)	0.205 (0.239)	0.304 (0.240)	0.330 (0.241)	0.229 (0.229)	0.242 (0.256)		-	-	-	-	-
WSV	0.186 (0.240)	0.131 (0.237)	0.187 (0.239)	0.289 (0.227)	0.368 (0.227)	0.336 (0.231)	0.246 (0.215)	0.204 (0.237)	0.990 (0.185) ^a		-	-	-	-
GAP	0.092 (0.135)	0.020 (0.129)	0.048 (0.138)	-0.201 (0.132)	-0.621 (0.106)	-0.653 (0.101)	-0.064 (0.143)	0.231 (0.137)	0.102 (0.327)	0.161 (0.314)		-	-	-
MelSc	-0.727 (0.373)	-0.804 (0.372)	-0.760 (0.375)	-0.577 (0.358)	0.043 (0.350)	0.156 (0.348)	-0.060 (0.321)	-0.876 (0.370)	-0.519 (0.913)	-0.451 (0.873)	0.341 (0.440)		-	-
PMel	-0.506 (0.247)	-0.594 (0.239)	-0.543 (0.244)	-0.460 (0.263)	0.071 (0.291)	0.012 (0.290)	-0.101 (0.261)	-0.809 (0.256)	-0.326 (0.546)	-0.303 (0.519)	0.074 (0.283)	0.999 (NE) ^a		-
FDef	0.217 (0.205)	0.144 (0.206)	0.258 (0.203)	0.272 (0.208)	0.071 (0.238)	0.177 (0.233)	0.345 (0.204)	0.062 (0.192)	-0.182 (0.432)	-0.233 (0.410)	0.343 (0.223)	0.446 (0.605)	0.276 (0.386)	

^a Estimates from bivariate models; NE=s.e. not estimabl

- Genetic parameters for CT-traits from dead and live fish scanning

CT phenotypes from the segmentation were expressed in volumes and for the genetic parameter estimation these phenotypes were converted into weight traits by multiplying the segmented tissue volumes with their corresponding densities: 1.354 kg/l , 1.067 kg/l and 0.933 kg/l for bone, meat and fat, respectively. Genetic parameters of phenotypes obtained with OTSU-method segmentation are presented in this report. Details of trait abbreviations and definitions are presented in Table 9.

Variance components and heritabilities were estimated using ASReml (Gilmore et al. 2009) and following linear univariate animal model:

$$\mathbf{y} = \mathbf{X}\mathbf{b} + \mathbf{Z}_A\mathbf{a} + \mathbf{Z}_C\mathbf{c} + \mathbf{e},$$

where, \mathbf{y} is the vector of the CT phenotypes (and registration weight and length in live fish CT data) ; \mathbf{b} is the vector of overall mean, fixed effects of sex, number of days from the start of the registration (live fish CT data) and tagging weight (live fish CT data); \mathbf{a} is the vector of random additive genetic effects; \mathbf{c} is the vector of random family, \mathbf{e} is the vector of random residual effects. The \mathbf{X} , \mathbf{Z}_A and \mathbf{Z}_C the incidence matrices assigning phenotypes to the vectors of fixed effects, additive genetic effects, and family effects, respectively. For genetic and phenotypic correlations within datasets, a bivariate animal model was used. For bivariate analysis random family effect was excluded from the model whereas all other model factors were identical as in univariate analysis.

Heritability estimates

Dead fish CT scanning

All estimates of heritability for the dead fish CT phenotypes (N=2012) were significantly different from zero (Table 10). Lowest heritabilities were estimated for weight of the bone fraction (0.13-0.14) and body height (0.17). High heritabilities were estimated for the fat percentage traits (0.48-0.59). For these traits, proportion of family variation was estimated to be zero, so this factor was excluded from the statistical model.

Live fish CT scanning

Similar to dead fish CT phenotypes, all estimates of heritability for live fish CT phenotypes (N=1425), were significantly different from zero (Table 11). Interestingly, high heritabilities for the bone fraction was estimated from live fish (0.44). In general, slightly higher heritability was estimated for live fish CT phenotypes than those from dead fish CT scanning, with exception of fat percentage phenotypes: 0.19-0.34 vs. 0.48-0.59. Some of the differences may arise from the different size of datasets, partly different genetic background of the fish, and differences in body weight at the registration time point. This said, it is possible that the dead fish scanning of deep-frozen and thawed fish may alter the x-absorption properties of the different tissues, in particular that of fat, being responsible for a part of the difference in the heritabilities for bone weight and fat percentages.

For live fish scanning phenotypes for different proportions were available for 951 individuals. Moderate heritabilities were estimated for all other traits than lloinmeatwt (0.14) and bellymeatwt (0.14). It is not clear why the heritability for lloinmeatwt and rloinmeatwt were on different level.

Table 9 Abbreviations and description of the phenotypic traits from CT scanning datasets of whole fish (dead and live fish) and proportions.

Trait	Abbreviation	Information on the trait
Whole fish		
Total weight	totwt	totbonewt+totfatwt+totmeatwt, in grams
Total bone weight	totbonewt	In grams
Total fat weight	totfatwt	In grams
Total meat weight	totmeatwt	In grams
Head-on-gutted weight	HOGwt	HOGbonewt+HOGfatwt+HOGmeatwt, in grams
Head-on-gutted bone weight	HOGbonewt	In grams
Head-on-gutted fat weight	HOGfatwt	In grams
Head-on-gutted meat weight	HOGmeatwt	In grams
Fillet weight	filletwt	filletfatwt+filletmeatwt, in grams
Fillet fat weight	filletfatwt	Both fillets, in grams
Fillet meat weight	filletmeatwt	Both fillets, in grams
Fat percentage total	fatpertot	totfatwt/totwt*100, in %
Intestine weight	intwt	totwt-HOGwt, in grams
Intestine fat weight	intfatwt	totfatwt-HOGfatwt, in grams
Fat percentage HOG	fatperHOG	HOGfatwt/HOGwt*100, in %
Fat percentage fillet	fatperfillet	filletfatwt/fatwt*100, in %
Length	length	In mm
Width	width	In mm
Height	height	In mm
Proportions		
Left loin meat weight	lloinmeatwt	In grams
Right loin meat weight	rloinmeatwt	In grams
Total loin meat weight	loinmeats	Lloinmeatwt+rloinmeatwt, in grams
Left loin fat weight	lloinfatwt	In grams
Right loin fat weight	rloinfatwt	In grams
Total loin fat weight	loinfats	lloinfatwt+rloinfatwt, in grams
Fat percentage loins	fatperloins	loinfats/(loinmeats+loinfats)*100, in %
Belly meat weight	bellymeatwt	In grams
Belly fat weight	bellyfatwt	In grams
NQC meat weight	NQCmeatwt	In grams
NQC fat weight	NQCfatwt	In grams
Tail meat weight	tailmeat	In grams
Tail fat weight	tailfatwt	In grams

Table 10 Variance components and heritability estimates for CT traits from dead fish scanning.

Trait	N	Genetic variation		Residual variation		Family variation		Variance ratios			
		σ^2	SE	σ^2	SE	σ^2	SE	h^2	SE	c^2	SE
totwt	2012	118269	45140.8	407979	27000.6	23356.3	16803.1	0.22	0.08	0.04	0.03
totbonewt	2012	150.917	70.1939	966.812	48.7796	46.5842	29.8617	0.13	0.06	0.04	0.03
totfatwt	2012	16770.3	6311.22	48931.6	3584.73	3003.84	2241.67	0.24	0.09	0.04	0.03
totmeatwt	2012	48961.7	18134.0	163123.	10845.9	8563.04	6638.02	0.22	0.08	0.04	0.03
HOGwt	2012	95270.7	35026.0	306657.	20790.3	16066.1	12750.9	0.23	0.08	0.04	0.03
HOGbone	2012	152.013	70.0521	45.2353	29.3736	45.2353	29.3736	0.14	0.06	0.04	0.03
HOGfat	2012	14460.6	4605.29	28796.6	2548.37	1394.14	1515.37	0.32	0.10	0.03	0.03
HOGmeat	2012	39184.6	14786.6	138453.	8943.99	6998.72	5467.75	0.21	0.08	0.04	0.03
filletwt	1923	69295.3	25953.3	227465.	15537.2	11587.0	9576.03	0.22	0.08	0.04	0.03
filletfatwt	1923	12180.1	3713.45	21834.3	2050.17	877.737	1202.38	0.35	0.10	0.03	0.03
filletmeatwt	1923	29631.1	11948.0	116696.	7357.88	6172.66	4572.34	0.19	0.08	0.04	0.03
intwt	2012	2220.99	906.526	8099.51	538.531	645.913	352.958	0.20	0.08	0.06	0.03
intfatwt	2012	1012.51	434.554	3446.47	250.107	315.401	167.766	0.21	0.04	0.07	0.04
fatpertot	2012	2.44437	0.39811	3.47124	0.26041	-	-	0.59	0.06	-	-
fatperHOG	2012	3.68191	0.56041	3.72244	0.34277	-	-	0.50	0.06	-	-
fatperfillet	1923	4.68763	0.71241	4.38113	0.43249	-	-	0.48	0.06	-	-
length	2012	348.453	126.251	1212.86	77.1539	34.3386	44.5956	0.22	0.08	0.02	0.03
width	2012	11.4764	4.44822	40.7028	2.66904	2.15967	1.66128	0.21	0.08	0.04	0.03
height	2012	39.2192	15.8142	184.438	10.2866	7.07231	6.14984	0.17	0.07	0.03	0.03

Table 11 Variance components and heritability estimates for CT traits from live fish scanning.

Trait	N	Genetic variation		Residual variation		Family variation		Variance ratios			
		σ^2	SE	σ^2	SE	σ^2	SE	h^2	SE	c^2	SE
totwt	1425	266271.	84799.7	544780.	50442.6	62771.3	27652.6	0.30	0.09	0.07	0.03
totbonewt	1425	639.730	161.957	729.687	91.5542	68.8481	41.7261	0.44	0.10	0.05	0.03
totfatwt	1425	34255.5	10045.6	67145.8	6065.56	6211.64	3153.12	0.32	0.08	0.06	0.03
totmeatwt	1425	99745.7	32811.1	221299	19741.2	23856.4	10843.8	0.29	0.09	0.07	0.03
HOGwt	1422	194862.	62256.2	405280.	37147.6	45096.3	20313.6	0.30	0.09	0.07	0.03
HOGbone	1422	621.634	156.978	716.890	88.8340	64.3744	40.4870	0.44	0.10	0.05	0.03
HOGfat	1422	20735.6	6063.04	38756.8	3622.13	3869.35	1887.49	0.33	0.09	0.06	0.03
HOGmeat	1422	82047.2	27625.3	188086.	16630.1	20567.7	9223.18	0.28	0.09	0.07	0.03
filletwt	1231	147403.	47549.4	291111.	28624.5	32040.3	16100.7	0.31	0.09	0.07	0.03
filletfatwt	1231	17075.5	4878.71	28741.6	2932.82	2717.72	1552.98	0.35	0.09	0.06	0.03
filletmeatwt	1231	70184.5	23958.8	150432	14492.5	16756.9	8295.50	0.30	0.09	0.07	0.04
intwt	1425	6199.01	1648.67	10469.6	990.501	691.668	470.522	0.36	0.08	0.04	0.03
intfatwt	1425	2886.98	769.861	5318.75	471.939	204.698	215.472	0.34	0.08	0.02	0.03
fatpertot	1425	4.93862	1.33116	20.7024	1.20996	-	-	0.19	0.05	-	-
fatperHOG	1422	4.82452	1.31458	10.0205	0.82746	0.343667	0.38185	0.32	0.08	0.02	0.03
fatperfillet	1231	6.73130	1.81927	12.6645	1.14611	0.305598	0.53614	0.34	0.08	0.02	0.03
length	1425	1157.43	352.875	2412.34	214.227	207.889	111.171	0.31	0.08	0.06	0.03
width	1425	27.0718	8.10533	60.0175	5.02239	3.96932	2.52823	0.30	0.08	0.04	0.03
height	1425	137.832	46.8816	383.133	29.7233	30.4765	16.0403	0.25	0.08	0.06	0.03

Table 12 Variance components and heritability estimates for CT proportion traits from live fish scanning.

Trait	N	Genetic variation		Residual variation		Family variation		Variance ratios			
		σ^2	SE	σ^2	SE	σ^2	SE	h^2	SE	c^2	SE
lloinmeatwt	951	1755.57	667.517	3651.05	406.576	376.493	238.287	0.30	0.11	0.07	0.04
rloinmeatwt	951	751.189	481.531	3884.46	325.878	641.059	238.312	0.14	0.09	0.12	0.04
loinmeats	951	4946.65	2269.11	13873.1	1411.30	2040.03	927.286	0.24	0.10	0.10	0.04
lloinfatwt	951	560.072	160.021	716.640	95.0451	61.2477	48.6093	0.42	0.10	0.05	0.04
rloinfatwt	951	472.548	135.014	680.201	82.4486	32.0065	41.034	0.40	0.10	0.03	0.03
loinfats	951	2051.80	579.605	2642.92	345.932	182.942	172.587	0.42	0.10	0.04	0.04
loinfatper	951	8.01296	1.70985	8.86324	1.15107	-	-	0.47	0.08	-	-
bellymeatwt	951	1247.04	825.854	6344.98	546.04	1037.6	400.618	0.14	0.09	0.12	0.05
bellyfatwt	951	1213.76	363.401	1950.55	224.718	108.619	115.552	0.37	0.10	0.03	0.04
NQCmeatwt	951	8475.08	3621.83	23155.9	2297.21	2428.91	1403.99	0.25	0.10	0.07	0.04
NQCfatwt	951	1765.14	602.437	3617.64	380.004	245.238	207.826	0.31	0.10	0.04	0.04
tailmeatwt	951	581.508	229.845	1731.38	154.846	117.037	90.7264	0.24	0.09	0.05	0.04
tailfatwt	951	65.1470	28.3248	201.122	18.5537	21.0869	11.5962	0.23	0.09	0.07	0.04

Genetic correlations within datasets

Dead fish and live fish CT scanning

Genetic and phenotypic correlations between traits within datasets (dead, live, proportions) are presented in Table 13, 14 and 15. Following general trends were observed in genetic correlations:

- Body weight CT traits were highly genetically correlated, in fact in most cases can be considered as genetically same traits.
- Fat percentages were moderately positively (unfavourably) correlated with weight phenotypes (total and meat weight).
- Fat percentages were highly correlated with fat weight traits.
- Fat percentage traits (whole, gutted, fillet) were highly correlated with each other.
- Body weight, length and height were genetically (close) identical (not presented).
- Intestinal fat weight was moderately (dead fish)/highly (live fish) and unfavourably correlated with weight traits.

Table 13 Genetic (upper diagonal) and phenotypic (lower diagonal) correlations for CT traits from dead fish scanning. Heritabilities on the diagonal are estimates from the univariate analysis.

Variable	totwt	totfatwt	totmeatwt	HOGwt	HOGfatwt	HOGmeatwt	Filletwt	filletfatwt	filletmeatwt	intwt	intfatwt	fatpertotal	fatperHOG	fatperfillet
Totwt	0.22 (0.08)	0.94 (0.01)	0.98 (0.00)	1.0 (0.00)	0.90 (0.02)	0.98 (0.01)	-	0.88 (0.03)	0.97 (0.01)	0.87 (0.03)	0.61 (0.07)	0.50 (0.09)	0.55 (0.08)	0.54 (0.08)
Totfatwt	0.95 (0.01)	0.24 (0.09)	0.86 (0.03)	0.93 (0.02)	0.97 (0.01)	0.85 (0.03)	0.94 (0.01)	0.96 (0.01)	0.84 (0.04)	0.84 (0.03)	0.62 (0.07)	0.77 (0.05)	0.77 (0.05)	0.76 (0.05)
totmeatwt	0.99 (0.00)	0.90 (0.01)	0.22 (0.08)	0.98 (0.00)	0.82 (0.04)	-	0.98 (0.01)	0.79 (0.04)	-	0.84 (0.04)	0.58 (0.08)	0.33 (0.11)	0.40 (0.10)	0.39 (0.10)
HOGwt	1.0 (0.00)	0.95 (0.00)	0.99 (0.00)	0.23 (0.08)	0.91 (0.02)	0.98 (0.01)	-	0.89 (0.02)	0.97 (0.01)	0.82 (0.04)	0.55 (0.08)	0.49 (0.09)	0.57 (0.08)	0.56 (0.08)
HOGfatwt	0.93 (0.00)	0.98 (0.00)	0.87 (0.01)	0.93 (0.00)	0.32 (0.10)	0.80 (0.04)	0.92 (0.02)	-	0.79 (0.05)	0.70 (0.06)	0.41 (0.10)	0.76 (0.05)	0.86 (0.03)	0.85 (0.03)
HOGmeatwt	0.98 (0.00)	0.89 (0.01)	-	0.99 (0.00)	0.86 (0.01)	0.21 (0.08)	0.97 (0.01)	0.77 (0.05)	-	0.83 (0.04)	0.59 (0.08)	0.31 (0.11)	0.38 (0.10)	0.36 (0.10)
filletwt	-	0.95 (0.00)	0.99 (0.00)	-	0.93 (0.00)	0.98 (0.00)	0.22 (0.08)	0.90 (0.02)	0.97 (0.01)	0.83 (0.04)	0.56 (0.08)	0.50 (0.09)	0.57 (0.08)	0.56 (0.08)
filletfatwt	0.91 (0.00)	0.98 (0.00)	0.85 (0.01)	0.92 (0.00)	-	0.84 (0.01)	0.92 (0.00)	0.35 (0.10)	0.77 (0.05)	0.68 (0.06)	0.39 (0.10)	0.77 (0.05)	0.87 (0.03)	0.87 (0.03)
filletmeatwt	0.98 (0.00)	0.88 (0.01)	-	0.98 (0.00)	0.84 (0.01)	-	0.98 (0.00)	0.83 (0.01)	0.19 (0.08)	0.84 (0.04)	0.60 (0.08)	0.30 (0.11)	0.35 (0.11)	0.34 (0.11)
intwt	0.92 (0.00)	0.90 (0.01)	0.90 (0.01)	0.89 (0.01)	0.82 (0.01)	0.89 (0.01)	0.89 (0.01)	0.80 (0.01)	0.89 (0.01)	0.20 (0.08)	0.89 (0.02)	0.51 (0.09)	0.36 (0.10)	0.34 (0.10)
intfatwt	0.79 (0.01)	0.80 (0.01)	0.76 (0.01)	0.76 (0.01)	0.67 (0.02)	0.77 (0.01)	0.77 (0.01)	0.66 (0.02)	0.77 (0.01)	0.93 (0.00)	0.21 (0.04)	0.44 (0.09)	0.13 (0.11)	0.11 (0.11)
fatpertotal	0.56 (0.02)	0.77 (0.01)	0.44 (0.02)	0.55 (0.02)	0.77 (0.01)	0.43 (0.02)	0.55 (0.02)	0.78 (0.01)	0.41 (0.02)	0.59 (0.02)	0.58 (0.02)	0.59 (0.06)	0.90 (0.02)	0.92 (0.00)
fatperHOG	0.56 (0.02)	0.75 (0.01)	0.45 (0.02)	0.57 (0.02)	0.82 (0.01)	0.43 (0.02)	0.57 (0.02)	0.83 (0.01)	0.41 (0.02)	0.48 (0.02)	0.36 (0.03)	0.93 (0.00)	0.50 (0.06)	-
fatperfillet	0.54 (0.02)	0.74 (0.01)	0.42 (0.02)	0.55 (0.02)	0.80 (0.01)	0.41 (0.02)	0.55 (0.02)	0.82 (0.01)	0.39 (0.02)	0.46 (0.02)	0.35 (0.03)	0.90 (0.02)	-	0.48 (0.06)

Table 14 Genetic (upper diagonal) and phenotypic (lower diagonal) correlations for CT traits from live fish scanning. Heritabilities on the diagonal are estimates from the univariate analysis.

Variable	totwt	totfatwt	totmeatwt	HOGwt	HOGfatwt	HOGmeatwt	Filletwt	filletfatwt	filletmeatwt	intwt	intfatwt	fatpertotal	fatperHOG	fatperfillet
Totwt	0.30 (0.09)	0.97 (0.01)	-	1.0 (0.00)	0.95 (0.01)	0.99 (0.00)	1.0 (0.00)	0.93 (0.02)	0.99 (0.00)	0.92 (0.02)	0.82 (0.05)	0.64 (0.11)	0.70 (0.07)	0.68 (0.08)
Totfatwt	0.95 (0.00)	0.32 (0.08)	0.93 (0.02)	0.97 (0.01)	0.98 (0.00)	0.93 (0.02)	0.97 (0.01)	0.98 (0.01)	0.93 (0.02)	0.90 (0.02)	0.82 (0.04)	0.83 (0.06)	0.83 (0.04)	0.82 (0.05)
totmeatwt	-	0.90 (0.01)	0.29 (0.09)	0.99 (0.00)	0.90 (0.03)	-	0.99 (0.00)	0.87 (0.01)	-	0.93 (0.02)	0.84 (0.04)	0.58 (0.11)	0.60 (0.09)	0.57 (0.10)
HOGwt	1.0 (0.00)	0.95 (0.00)	0.99 (0.00)	0.30 (0.09)	0.95 (0.01)	0.99 (0.00)	-	0.93 (0.02)	0.99 (0.00)	0.92 (0.02)	0.83 (0.04)	0.69 (0.09)	0.71 (0.07)	0.68 (0.08)
HOGfatwt	0.94 (0.00)	0.99 (0.00)	0.88 (0.01)	0.94 (0.00)	0.33 (0.09)	0.90 (0.03)	0.95 (0.01)	-	0.89 (0.03)	0.83 (0.04)	0.74 (0.06)	0.87 (0.04)	0.90 (0.03)	0.89 (0.03)
HOGmeatwt	0.99 (0.00)	0.90 (0.01)	-	0.99 (0.00)	0.89 (0.01)	0.28 (0.09)	0.99 (0.00)	0.87 (0.03)	0.99 (0.01)	0.92 (0.02)	0.84 (0.04)	0.58 (0.11)	0.60 (0.09)	0.57 (0.10)
filletwt	1.0 (ne)	0.95 (0.00)	0.99 (0.00)	-	0.94 (0.00)	0.99 (0.00)	0.31 (0.09)	0.94 (0.02)	0.99 (0.00)	0.92 (0.02)	0.83 (0.04)	0.70 (0.09)	0.71 (0.07)	0.69 (0.08)
filletfatwt	0.93 (0.00)	0.99 (0.00)	0.87 (0.03)	0.93 (0.00)	-	0.87 (0.01)	0.93 (0.00)	0.35 (0.09)	0.87 (0.04)	0.80 (0.05)	0.72 (0.06)	0.87 (0.04)	0.91 (0.03)	0.91 (0.03)
filletmeatwt	0.99 (0.00)	0.90 (0.01)	-	0.99 (0.00)	0.88 (0.01)	1.0 (0.00)	0.99 (0.00)	0.86 (0.01)	0.30 (0.09)	0.93 (0.02)	0.85 (0.04)	0.59 (0.11)	0.59 (0.10)	0.57 (0.10)
intwt	0.91 (0.01)	0.92 (0.01)	0.94 (0.00)	0.95 (0.00)	0.89 (0.01)	0.94 (0.00)	0.95 (0.00)	0.88 (0.01)	0.94 (0.00)	0.36 (0.08)	0.96 (0.01)	0.64 (0.10)	0.54 (0.10)	0.51 (0.10)
intfatwt	0.79 (0.01)	0.86 (0.01)	0.85 (0.01)	0.88 (0.00)	0.85 (0.01)	0.86 (0.01)	0.89 (0.01)	0.85 (0.01)	0.87 (0.01)	0.94 (0.00)	0.34 (0.08)	0.67 (0.09)	0.46 (0.11)	0.45 (0.11)
fatpertotal	0.46 (0.02)	0.67 (0.02)	0.62 (0.02)	0.72 (0.02)	0.87 (0.01)	0.63 (0.02)	0.74 (0.02)	0.88 (0.01)	0.64 (0.02)	0.67 (0.02)	0.77 (0.02)	0.19 (0.05)	0.95 (0.02)	0.94 (0.02)
fatperHOG	0.68 (0.02)	0.84 (0.01)	0.57 (0.02)	0.68 (0.02)	0.86 (0.01)	0.57 (0.02)	0.69 (0.02)	0.88 (0.01)	0.58 (0.02)	0.66 (0.02)	0.69 (0.02)	0.98 (0.00)	0.32 (0.08)	-
fatperfillet	0.68 (0.02)	0.83 (0.01)	0.57 (0.02)	0.68 (0.02)	0.86 (0.01)	0.57 (0.02)	0.68 (0.02)	0.87 (0.01)	0.56 (0.02)	0.66 (0.02)	0.68 (0.02)	0.97 (0.00)	-	0.34 (0.08)

Table 15 Genetic (upper diagonal) and phenotypic (lower diagonal) correlations for CT proportion traits from live fish scanning. Heritabilities on the diagonal are estimates from the univariate analysis.

Variable	lloinmeatwt	rloinmeatwt	loinmeats	lloinfatwt	rloinfatwt	loinfats	loinfatper	bellymeatwt	bellyfatwt	NQCmeatwt	NQCfatwt	tailmeatwt	tailfatwt
lloinmeatwt	0.30 (0.11)	0.99 (0.01)	-	0.88 (0.04)	0.90 (0.04)	0.89 (0.04)	0.59 (0.11)	0.98 (0.01)	0.91 (0.04)	0.96 (0.02)	0.89 (0.04)	0.86 (0.05)	0.90 (0.04)
rloinmeatwt	0.89 (0.01)	0.14 (0.09)	-	0.84 (0.05)	0.85 (0.05)	0.85 (0.05)	0.49 (0.12)	0.99 (0.01)	0.84 (0.06)	0.97 (0.02)	0.85 (0.05)	0.93 (0.04)	0.89 (0.04)
loinmeats	-	-	0.24 (0.10)	0.85 (0.04)	0.87 (0.04)	0.86 (0.04)	0.53 (0.11)	0.98 (0.01)	0.87 (0.04)	0.96 (0.02)	0.87 (0.05)	0.89 (0.04)	0.89 (0.04)
lloinfatwt	0.84 (0.01)	0.82 (0.01)	0.85 (0.01)	0.42 (0.10)	0.99 (0.01)	-	0.89 (0.03)	0.78 (0.07)	0.98 (0.01)	0.83 (0.05)	0.98 (0.01)	0.80 (0.07)	0.94 (0.02)
rloinfatwt	0.80 (0.01)	0.84 (0.01)	0.84 (0.01)	0.94 (0.00)	0.40 (0.10)	-	0.88 (0.04)	0.80 (0.07)	0.98 (0.01)	0.83 (0.05)	0.98 (0.01)	0.81 (0.07)	0.94 (0.02)
loinfats	0.83 (0.01)	0.84 (0.01)	0.86 (0.01)	-	-	0.42 (0.10)	0.89 (0.03)	0.79 (0.07)	0.99 (0.01)	0.83 (0.05)	0.98 (0.01)	0.80 (0.07)	0.94 (0.02)
loinfatper	0.54 (0.03)	0.56 (0.03)	0.56 (0.03)	0.86 (0.01)	0.86 (0.01)	0.87 (0.01)	0.47 (0.08)	0.40 (0.14)	0.86 (0.04)	0.53 (0.11)	0.87 (0.04)	0.52 (0.13)	0.76 (0.07)
bellymeatwt	0.88 (0.01)	0.91 (0.01)	0.92 (0.01)	0.75 (0.02)	0.73 (0.02)	0.75 (0.02)	0.43 (0.03)	0.14 (0.09)	0.77 (0.07)	0.97 (0.02)	0.79 (0.07)	0.89 (0.05)	0.82 (0.06)
bellyfatwt	0.77 (0.02)	0.79 (0.01)	0.80 (0.01)	0.94 (0.00)	0.93 (0.00)	0.95 (0.00)	0.85 (0.01)	0.71 (0.02)	0.37 (0.10)	0.81 (0.06)	0.96 (0.02)	0.83 (0.07)	0.93 (0.03)
NQCmeatwt	0.89 (0.01)	0.90 (0.01)	0.92 (0.01)	0.80 (0.01)	0.81 (0.01)	0.82 (0.01)	0.57 (0.03)	0.86 (0.01)	0.70 (0.02)	0.25 (0.10)	0.86 (0.05)	0.82 (0.06)	0.85 (0.05)
NQCfatwt	0.77 (0.02)	0.79 (0.01)	0.80 (0.01)	0.93 (0.01)	0.93 (0.01)	0.94 (0.00)	0.86 (0.01)	0.66 (0.02)	0.87 (0.01)	0.84 (0.01)	0.31 (0.10)	0.77 (0.09)	0.95 (0.03)
tailmeatwt	0.77 (0.01)	0.79 (0.01)	0.80 (0.01)	0.67 (0.02)	0.64 (0.02)	0.66 (0.02)	0.40 (0.03)	0.80 (0.01)	0.60 (0.02)	0.74 (0.02)	0.61 (0.02)	0.24 (0.09)	0.91 (0.04)
tailfatwt	0.82 (0.01)	0.85 (0.01)	0.85 (0.01)	0.88 (0.01)	0.89 (0.01)	0.90 (0.01)	0.73 (0.02)	0.81 (0.01)	0.85 (0.01)	0.80 (0.01)	0.83 (0.01)	0.78 (0.01)	0.23 (0.09)

5.4.2 Genetic correlation manual vs CT on dead and live fish

To validate how well CT scan phenotypes as reflect the dissection phenotypes, genetic correlations were estimated between some of the phenotypes registered from same individuals: dead fish dissection and CT scanning. Table 16 summarizes the results from this assessment.

Table 16 Genetic (upper diagonal) and phenotypic (lower diagonal) correlations for CT traits from dead fish scanning.

Variable	HWT*	FWT*	FAT*	filletwt	filletfatwt	fatperfillet	intfatwt
HWT*		0.89 (0.02)	0.35 (0.09)	-	0.92 (0.02)	0.61 (0.07)	0.69 (0.06)
FWT *	0.90 (0.00)		0.65 (0.06)	1.0 (0.00)	0.95 (0.01)	0.68 (0.06)	0.72 (0.05)
FAT *	0.37 (0.02)	0.43 (0.02)		0.64 (0.08)	0.85 (0.04)	0.91 (0.03)	0.21 (0.12)
Filletwt	-	0.94 (0.00)	0.52 (0.02)		0.90 (0.02)	0.56 (0.08)	0.56 (0.08)
filletfatwt	0.91 (0.00)	0.88 (0.01)	0.65 (0.02)	0.92 (0.02)		0.87 (0.03)	0.39 (0.10)
fatperfillet	0.57 (0.02)	0.57 (0.02)	0.67 (0.02)	0.55 (0.02)	0.82 (0.01)		0.11 (0.11)
intfatwt	0.80 (0.01)	0.75 (0.01)	0.39 (0.03)	0.77 (0.01)	0.66 (0.02)	0.35 (0.03)	

*HWT, FWT and FAT are traits from the manual slaughter

Manual weight traits (HWT, FWT) and filletwt from CT are genetically same trait. This (and results above) confirms that genetic improvement of fillet yield is difficult when selection is based on harvest weight. Fatperfillet was moderately genetically correlated with HWT, FWT and filletwt (0.56-0.68). High genetic correlation between fat content phenotypes from manual dissection (NIR) and CT confirm close to identical ranking of individuals based on the two phenotypes. All weight traits are unfavourable correlated with the weight of abdominal fat, with exception of fatperfillet where correlation was not significantly different from zero. This result was not confirmed in live fish CT scanning (0.45, Table 14).

An attempt was made to connect the manual slaughter dissection traits with the CT phenotypes from the live fish CT scanning. Unfortunately, due to the technical complications (see Section 5.1.1) the live fish scanned were more remotely related to the manual dissection and dead fish CT data than originally planned (Table 2). This resulted in very weak pedigree links between the two datasets and estimation of genetic correlations based on pedigree was not successful. No genomic links could be formed as the genotyping of the individuals of the manual slaughter failed.

5.4.3 Genome-wide association study and genomic analysis of live fish CT scans

Genomic analysis was performed for a selection of the original unconverted volume traits from the live fish scanning, as no genomic information was available for the dead fish dataset.

Following the collection of the adipose fin-clips, samples were sent to IdentiGEN (<https://identigen.com/>; Dublin, Ireland) for DNA extraction and genotyping. Genotyping was done on a custom-made, 55 K Affymetrix Axiom array. The initial quality control and SNP calling steps were done with the Affymetrix Axiom analysis suite software. Additional filtering was implemented using PLINK version 1.9 where we removed the low-quality genotyped samples and SNPs by setting call rates < 95 %, Hardy-Weinberg p -value < 10^{-10} and minor allele frequency < 0.05 %. The estimation of variance components and SNP-based heritability, as well as the genome-wide association study (GWAS), was performed using restricted maximum likelihood and mixed linear

model, implemented in GCTA v1.93. The model used for estimating variance components for was as follows:

$$y = Xb + Z_1c + Z_2g + e$$

where y is the vector of the phenotype, X , Z_1 and Z_2 are the incidence matrices assigning phenotype to the vectors of fixed effects (b), i.e., tag weight and the gender effect, predicted based on the presence or absence of Y-specific genetic markers, the common-environmental family effect (c), the animal effect (g) and the residuals (e). The effects common to families, animal and residuals are assumed to follow a normal distribution, i.e., $cN(0, I\sigma_c^2)$, $uN(0, G\sigma_g^2)$ and $eN(0, I\sigma_e^2)$, where I is an identity matrix, G is the genomic relationship matrix, σ_c^2 , σ_g^2 and σ_e^2 are the variances of full-sib family effect, additive genetic and residuals.

Results from the live fish sampling

Phenotypic correlations between the traits analysed with GWAS are shown in Figure 25. Many traits have correlations close to 1 (> 0.75), indicating that a number of these traits are providing us the same information.

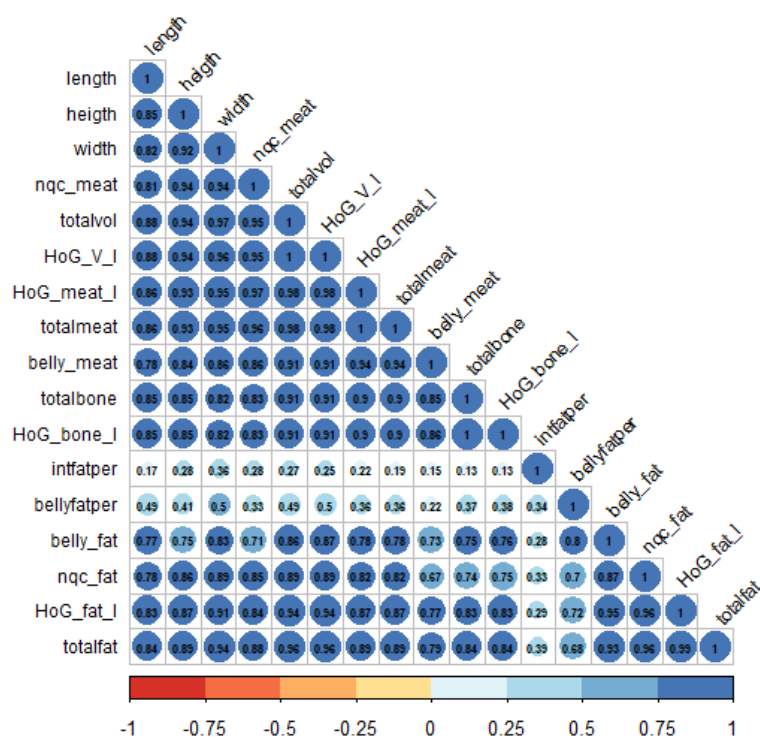


Figure 25 Phenotypic correlations between some of the CT measured phenotypes from live fish recording.

In total, 47,945 SNPs passed the genotyping quality control steps. GWAS was performed on number of traits. Figure 26 shows a selection of Manhattan plots from six traits: total volume, total fat, total meat, width, length and height. The overall similarity in the patterns of associations among these phenotypes, with a peak on chromosome 9, might be reflection of high correlation between these traits. Following the variance components for the same traits are given in Table 17. These estimates are slightly higher but aligned with the estimates based on pedigree information only (Table 11).

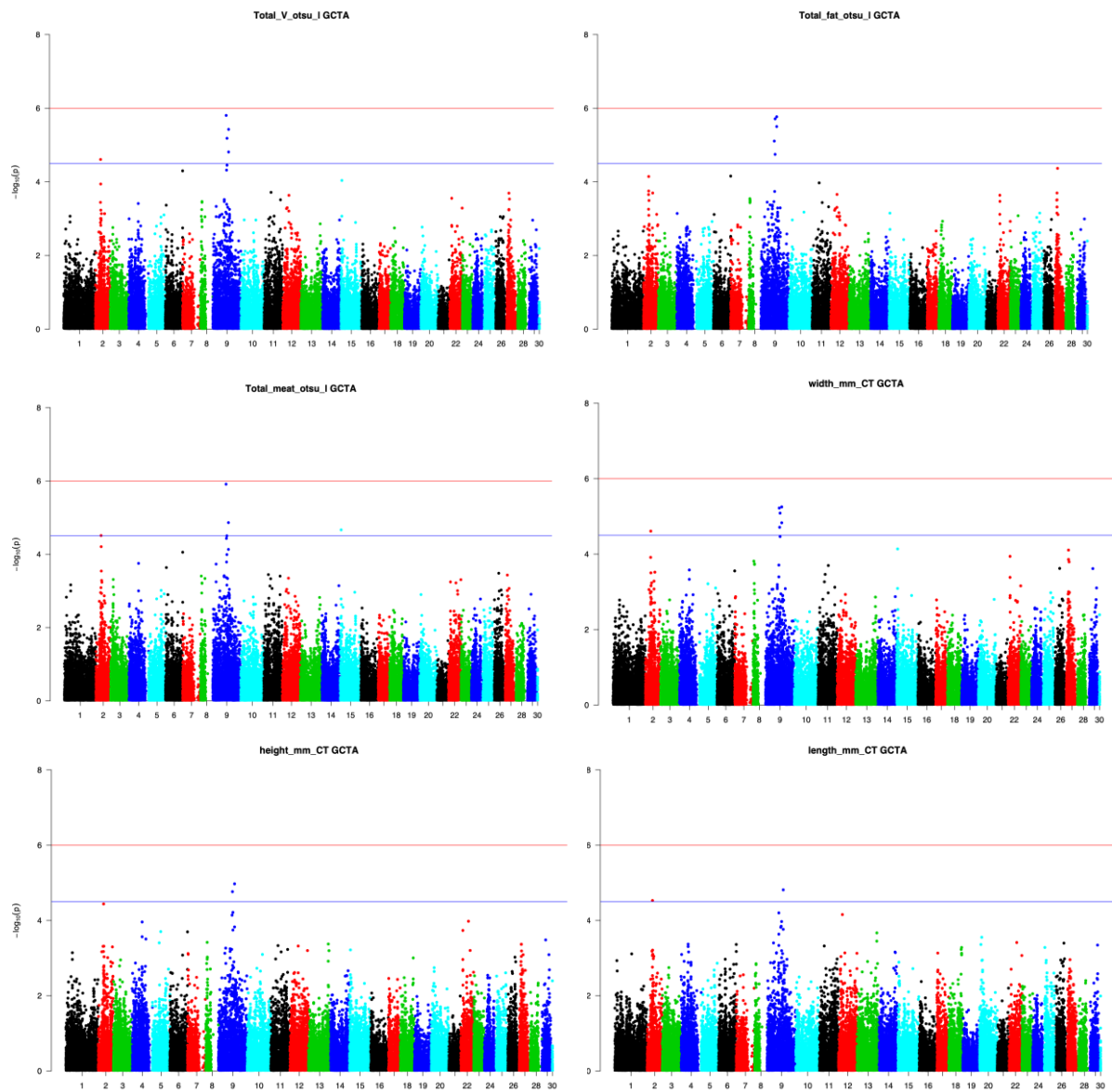


Figure 26 *Manhattan plots from GWAS analyses for total volume, total meat, height (left panels from top), total fat, width and length (right panels from top) measured on live fish using CT scanner.*

Table 17 Variance components for six CT measured traits: total volume of the fish, total meat content, total fat content, width, height, and length.

Trait	N	Genetic variation		Residual variation		Phenotypic variation		Heritability	
		σ^2	SE	σ^2	SE	σ^2	SE	h^2	SE
Total volume (l)	1255	0.30	0.05	0.52	0.03	0.82	0.04	0.37	0.05
Total meat (l)	1255	0.11	0.02	0.20	0.01	0.31	0.01	0.35	0.05
Total fat (l)	1255	0.05	0.01	0.08	0.00	0.12	0.01	0.37	0.05
Width	1258	27.48	4.86	63.39	3.57	90.87	4.25	0.30	0.05
Height	1258	171.72	30.06	378.89	21.58	550.61	25.99	0.31	0.05
Length	1258	1238	206	2526	144	2764	178	0.32	0.04

5.4.4 Discussion and conclusions for WP4

CT traits from dead fish and live fish scanning showed promised for genetic improvement on CT phenotypes. Estimates from the two datasets were moderate, ranging between 0.19-0.44 with exceptions of low heritability estimated for bone fraction (0.13-0.14) and height of the fish (0.17) and high heritability for fat percentages of round and gutted fish, as well as in fillet (0.48-0.59) in dead fish scanning. CT scanning reliably reflects the body composition of salmon, verified by high phenotypic and genetic correlations between corresponding traits. GWAS did not indicate any large QTLs for the investigated traits, but rather confirmed the strong genetic interrelationships between weight traits and morphology.

6 Main findings

- CT scanning and consequent custom-made segmentation of live fish CT scans provides accurate and highly heritable CT phenotypes that can be used as selection criteria for body composition and slaughter quality for increase genetic gain. Method enables definition of novel post-scan phenotypes using same CT scans.
- Fillet quality traits, melanin spots, gaping and pigmentation, were not detectable in CT scanning.
- Manually registered melanin spots showed zero heritability.
- NIR scanning of salmon muscle sides is expectedly robust for quantification of fat and pigments, whereas novel approaches of NIR based Qpoint or handheld SORS device failed to quantify pigmentation in whole fish.

7 Deliverables

Deliverables following description in the FHF project plan delivered as follows. Changes after the amendment marked on red.

Minutes of the meetings:

- Kick-off meeting 2018, February 22nd
- Reference group meetings:
 - 2018, June 6th, October 25th
 - 2019, February 22nd, June 5th and October 1st
 - 2020: January 27th (was changed into ordinary reference group meeting), May 6th (final reference group meeting postponed according to amendment)

Oral/poster presentations:

- Oral presentation: “Towards industrial analysis of quality parameters in intact salmon using spatially offset Raman spectroscopy”, SpringSciX, Glasgow, 2018, April 20th
- Oral presentation in the Aquaculture Europe conference, Berlin, 2019, October 10th
- Oral presentation in digital HAVBRUK 2020, June 9th
- Poster presentation in the 6th International Symposium on Genomics in Aquaculture, GIA 2020 (conference postponed until September due to Covid19)

Popular scientific articles:

- Norsk Fiskeoppdrett N:o 3, 2018, 12-14. CT-skanner avls-laksen for å finne de beste individene
- Advertisement article kyst.no
- <https://www.kyst.no/advertisement/kan-problemet-med-melaninflekker-loeses-gjennom-avl/>

Scientific papers, manuscripts by 1.9.2020

- Nielsen D.B. et al. Potential of using CT scans to quantify quality traits in Atlantic salmon
- Afseth, N.K., et al. The potential of Raman spectroscopy for probing quality features of intact fish
- Kettunen et al. Genetic parameters for body composition and slaughter quality of dead and alive Atlantic salmon using computer tomography
- Hillestad B. et al. Genome-wide association study for quality traits in Atlantic salmon using CT

Reports and amendments:

- Periodic report submitted 2018, December 31st
- Amendment, submitted November 28th
- Project status reporting and minutes of the extraordinary reference group meeting 2020, January 27th was considered as status reporting 2019
- Final scientific and administrative report submitted 2020, June 19th

8 Acknowledgements

Thank you for Arnaud Lefrancois for analysing and developing the wound scoring scheme. We thank Karen Wahlstrøm Sanden and Ulrike Böcker at Nofima for their efforts and expertise on VIS/NIR and Raman measurements on site and in laboratory.

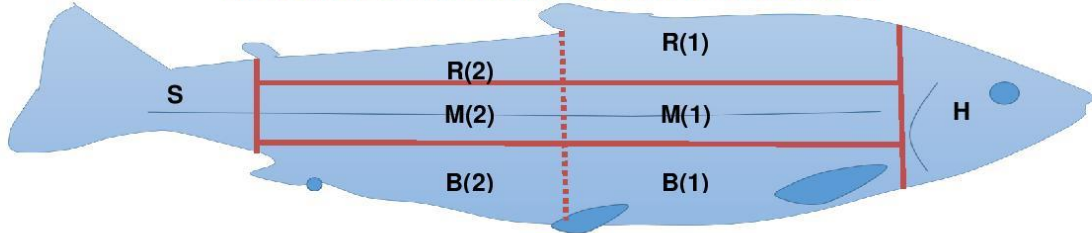
9 Literature

- Afseth, NK, M Bloomfield, Jens Petter Wold, and P Matousek. 2014. 'A Novel Approach for Subsurface Through-Skin Analysis of Intact Salmon Using Spatially Offset Raman Spectroscopy (SORS)'. *Applied Spectroscopy* 68 (2): 255–62.
- Andersen, UB, AN Strømsnes, K Steinsholt, and MS Thomassen. 1994. 'Fillet Gaping in Farmed Atlantic Salmon'. *Norwegian Journal of Agricultural Science* 8: 165–79.
- Gilmour, A, BJ Gogel, BR Cullis, and R Thompson. 2009. 'ASReml User Guide Release 3.0.' Hemel Hempstead, HP1 1ES, UK: VSN International Ltd.
- Gjerde, Bjarne. 1987. 'Predicting Carcass Composition of Rainbow Trout by Computerized Tomography'. *Journal of Animal Breeding and Genetics* 104: 121–36.
- Gjerlaug-Enger, E, J Kongsro, J Odegård, L Aass, and O Vangen. 2012. 'Genetic Parameters between Slaughter Pig Efficiency and Growth Rate of Different Body Tissues Estimated by Computed Tomography in Live Boars of Landrace and Duroc.' *Animal* 6 (1): 9–18.
- Heia, K, Jens Petter Wold, and Martin Hansen Skjelvareid. 2016. 'Metoder for Kvalitetsmåling På Hel Laks'. 7. Nofima Rapport.
- Holló, G, B Húth, E Egri, I Holló, and I Anton. 2017. 'Intramuscular Connective Tissue Properties in Longissimus Thoracis Muscle of Simmental Cattle.' *Advances in Animal Biosciences* 8 (48–50).
- Maximini, L, DJ Brown, R Baumung, and B Fuerst-Waltl. 2012. 'Genetic Parameters of Ultrasound and Computer Tomography Scan Traits in Austrian Meat Sheep.' *Livestock Science* 146 (2–3): 168–74.
- Rye, Morten. 1991. 'Prediction of Carcass Composition in Atlantic Salmon by Computerized Tomography'. *Aquaculture* 99: 35–48.

ARNAUD'S WOUND SCALE

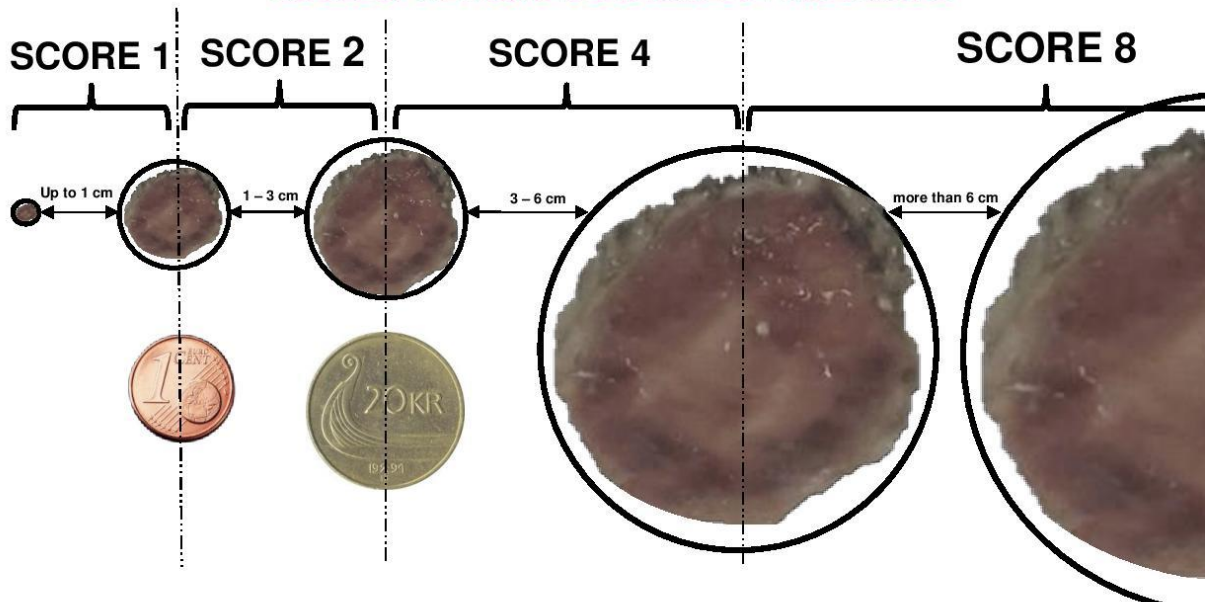
POSITION

THE CENTER OF THE WOUND DETERMINES THE POSITION

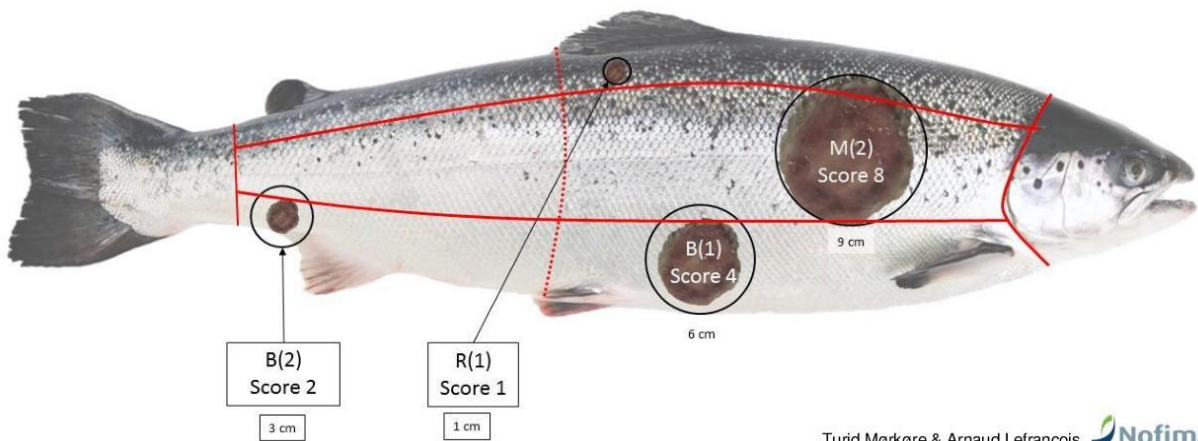


SIZE

THE SIZE OF THE WOUND IS DETERMINED BY THE DIAMETER



EXAMPLE



Appendix 2. Dicom header for CT scanning.

Dicom header

[0008,0000]	GenericGroupLength	360	UL	4		
[0008,0008]	ImageType [3]	ORIGINAL, PRIMARY, AXIAL	CS	22		
[0008,0016]	SOPClassUID	1.2.840.10008.5.1.4.1.1.2	UI	26		
[0008,0018]	SOPInstanceUID	1.2.392.200036.9116.2.5.1.16.1613454497.1520322637.721630	UI	58		
[0008,0020]	StudyDate	20180306	DA	8		
[0008,0022]	AcquisitionDate	20180306	DA	8		
[0008,0023]	ContentDate	20180306	DA	8		
[0008,0030]	StudyTime	084210.000	TM	10		
[0008,0032]	AcquisitionTime	084225.000	TM	10		
[0008,0033]	ContentTime	084225.812	TM	10		
[0008,0050]	AccessionNumber	1987	SH	4		
[0008,0060]	Modality	CT	CS	2		
[0008,0070]	Manufacturer	TOSHIBA	LO	8		
[0008,0080]	InstitutionName	DMRI	LO	4		
[0008,0090]	ReferringPhysicianName		PN	0		
[0008,1010]	StationName	ID_STATION	SH	10		
[0008,103e]	SeriesDescription	//FC01	LO	6		
[0008,1040]	InstitutionalDepartmentName	ID_DEPARTMENT	LO	14		
[0008,1090]	ManufacturerModelName	Aquilion	LO	8		
[0010,0000]	GenericGroupLength	38	UL	4		
[0010,0010]	PatientName	a	PN	2		
[0010,0020]	PatientID	6836	LO	4		
[0010,0030]	PatientBirthDate		DA	0		
[0010,0040]	PatientSex		CS	0		
[0018,0000]	GenericGroupLength	234	UL	4		
[0018,0022]	ScanOptions	HELICAL_CT	CS	10		
[0018,0050]	SliceThickness	2.0	DS	4		
[0018,0060]	KVP	100	DS	4		
[0018,0090]	DataCollectionDiameter	400.00	DS	6		
[0018,1000]	DeviceSerialNumber	GCB06Y2751	LO	10		
[0018,1020]	SoftwareVersions	V1.62GR502	LO	10		
[0018,1030]	ProtocolName	FishScan0.75_100_150_2mm	LO	24		
[0018,1100]	ReconstructionDiameter	400.00	DS	6		
[0018,1120]	GantryDetectorTilt	+0.0	DS	4		
[0018,1130]	TableHeight	+61.00	DS	6		
[0018,1140]	RotationDirection	CW	CS	2		
[0018,1150]	ExposureTime	750	IS	4		
[0018,1151]	XRayTubeCurrent	150	IS	4		
[0018,1152]	Exposure	112	IS	4		
[0018,1210]	ConvolutionKernel	FC01	SH	4		
[0018,5100]	PatientPosition	HFS	CS	4		
[0020,0000]	GenericGroupLength	380	UL	4		
[0020,000d]	StudyInstanceUID	1.2.392.200036.9116.2.5.1.16.1613454497.1520322076.877093	UI	58		
[0020,000e]	SeriesInstanceUID	1.2.392.200036.9116.2.5.1.16.1613454497.1520322637.718486	UI	58		
[0020,0010]	StudyID	1987	SH	4		

[0020,0011]	SeriesNumber	1	IS	2		
[0020,0012]	AcquisitionNumber	1	IS	2		
[0020,0013]	InstanceNumber	1	IS	2		
[0020,0020]	PatientOrientation	[2] L, P	CS	4		
[0020,0032]	ImagePositionPatient	[3] -200.000000, -200.000000, -899.500000			DS	36
[0020,0037]	ImageOrientationPatient	[6] 1.000000, 0.000000, 0.000000, 0.000000, 1.000000, 0.000000			DS	54
[0020,0052]	FrameOfReferenceUID	1.2.392.200036.9116.2.5.1.16.1613454497.1520322131.101631			UI	58
[0020,1040]	PositionReferenceIndicator		LO	0		
[0020,1041]	SliceLocation	+0.00	DS	6		
[0028,0000]	GenericGroupLength	152	UL	4		
[0028,0002]	SamplesPerPixel	1	US	2		
[0028,0004]	PhotometricInterpretation		MONOCHROME2	CS	12	
[0028,0010]	Rows	512	US	2		
[0028,0011]	Columns	512	US	2		
[0028,0030]	PixelSpacing	[2] 0.781, 0.781	DS	12		
[0028,0100]	BitsAllocated	16	US	2		
[0028,0101]	BitsStored	16	US	2		
[0028,0102]	HighBit	15	US	2		
[0028,0103]	PixelRepresentation	1	US	2		
[0028,1050]	WindowCenter	40	DS	2		
[0028,1051]	WindowWidth	300	DS	4		
[0028,1052]	RescaleIntercept	0	DS	2		
[0028,1053]	RescaleSlope	1	DS	2		
[0040,0000]	GenericGroupLength	116	UL	4		
[0040,0002]	ScheduledProcedureStepStartDate	20180306	DA	8		
[0040,0003]	ScheduledProcedureStepStartTime	084210.000	TM	10		
[0040,0004]	ScheduledProcedureStepEndDate	20180306	DA	8		
[0040,0005]	ScheduledProcedureStepEndTime	090210.000	TM	10		
[0040,0244]	PerformedProcedureStepStartDate	20180306	DA	8		
[0040,0245]	PerformedProcedureStepStartTime	084210.000	TM	10		
[0040,0253]	PerformedProcedureStepID	25491	SH	6		
[7005,0000]	PrivateGroupLength	182	UL	4		
[7005,0010]	PrivateCreator	TOSHIBA_MEC_CT3	LO	16		
[7005,1008]	Unknown Tag & Data	32	??	4		
[7005,1009]	Unknown Tag & Data	30	??	16		
[7005,100a]	Unknown Tag & Data	2d	??	6		
[7005,100b]	Unknown Tag & Data	4f	??	4		
[7005,100e]	Unknown Tag & Data	49	??	4		
[7005,100f]	Unknown Tag & Data	48	??	2		
[7005,1012]	Unknown Tag & Data	53	??	2		
[7005,1013]	Unknown Tag & Data	01	??	2		
[7005,101d]	Unknown Tag & Data	01	??	4		
[7005,1022]	Unknown Tag & Data	32	??	4		
[7005,1023]	Unknown Tag & Data	31	??	6		
[7005,1024]	Unknown Tag & Data	32	??	8		
[7fe0,0000]	GenericGroupLength	524296	UL	4		
[7fe0,0010]	PixelData	f800	OW	524288		

